Research Article

An Efficient Approach to the Simulation-Based Sensitivity Analysis of Building Performance: OPAT-based LSA and Sobol-based GSA

Masoud Nasouri^{1*}, Navid Delgarm^{2} ID

^{1}Department of Environment, Aras International Campus, University of Tehran, Tehran, Iran
^{2}Department of Mechanical and Aerospace Engineering, Malek-Ashtar University of Technology, Isfahan, Iran
 Email: M.Nasouri@ut.ac.ir

Abstract: This work presents a new efficient approach to the simulation-based sensitivity analysis (SBSA) of building performance. To this end, through a new initiative, the whole building energy simulation program EnergyPlus is combined with the local sensitivity analysis (LSA) and global sensitivity analysis (GSA) through the C++ programming language. The developed method is applied to a dwelling house in the hot semi-arid climate region of Iran. Hereupon, the building design parameters including BR, WWR, DSH, CSPT, HSPT, $SA_{\text{IN\_W}}$, $SA_{\text{Ex\_W}}$, $Th_{\text{Ex\_W}}$, ST_{win}, VT_{win}, Th_{win}, and $Th_{gas\text{-}win}$ are adopted as input variables. Moreover, four major building criteria including annual heating energy consumption (AHC), annual cooling energy consumption (ACC), annual lighting energy consumption (ALC), and predicted percentage of dissatisfied (PPD) index are adopted as output variables. The one-parameter-at-a-time (OPAT) as the LSA and Sobol's analysis as the GSA are carried out to explore the behavior of outputs versus inputs changes and to quantify the total sensitivity of outputs-to-inputs (S_T). In the LSA approach, a new sensitivity indicator called the Dispersion Index (DI) is proposed to define the influence of inputs on outputs. The results demonstrate that for our typical building under study, AHC is most sensitive to the HSPT and $SA_{\text{Ex\_W}}$, with S_T of respectively 80% and 79%. While ACC is most sensitive to the CSPT and $SA_{\text{Ex\_W}}$ with S_T of respectively 72% and 63%. Besides, WWR, VT_{win}, and BR with S_T of respectively 33%, 25%, and 21% are the most influential inputs on the ALC. Furthermore, CSPT, HSPT, $SA_{\text{Ex\_W}}$, and WWR with S_T of respectively 81%, 40%, 36%, and 21% are the most influential inputs on the PPD. ALC has no dependence on the CSPT and HSPT of VAV and thermo-physical traits of wall and window. Besides, the sensitivity results obtained by the proposed DI in OPAT-based LSA are in good accordance with the Sobol-based GSA ones.

Keywords: simulation-based sensitivity analysis, coupling framework, OPAT analysis, Sobol's analysis, building efficiency, thermal comfort

Nomenclature

ACC	Annual cooling energy consumption	OPAT	One-parameter-at-a-time
AHC	Annual heating energy consumption	PCM	Phase change material

ALC	Annual lighting energy consumption	PMV	Predicted mean vote
ATC	Annual total energy consumption	PPD	Predicted percentage of dissatisfied
BEMT	Building Energy Modeling Tool	SA	Sensitivity analysis
BF	Building facade	SA_{Ex_W}	Solar absorptance of the exterior wall
BPA	Building Performance Analysis	SA_{IN_W}	Solar absorptance of the interior wall
BR	Building rotation	SALib	Sensitivity analysis library
BTO	Building Technologies Office	DSH	Depth of shading device
CDD	Cooling degree-day	SI	Sensitivity index
CSPT	Cooling setpoint temperature	SBSA	Simulation-based sensitivity analysis
DI	Dispersion Index	S_T	Total-order sensitivity index
DOE	Department of Energy	ST_{win}	Solar transmittance of window glass
GSA	Global sensitivity analysis	Th_{Ex_W}	Thickness of wall
HDD	Heating degree-day	$Th_{gas-win}$	Thickness of gas in window
HSPT	Heating setpoint temperature	Th_{win}	Thickness of window glass
HVAC	Heating, ventilation, and air conditioning	VAV	Variable air volume
LSA	Local sensitivity analysis	VT_{win}	Visible transmittance of window glass
MIP	Mixed-integer programming	WWR	Window-to-wall ratio

1. Introduction

In Iran, the buildings are responsible for about 38% of total energy consumption and 33% of total CO_2 emissions as a result of the burning fossil fuels for the production of heat and power as well as the production of materials such as cement, steel, and aluminum utilized for construction of buildings [1], [2]. According to the Ministry of Energy of Iran [3], the share of energy use in the building sector is 3 to 5 times larger than the world average. Further, the energy intensity per capita in Iran is about 2 times larger than the global rates [4]. Increasing costs and demand for energy in the building sector have caused building designers and energy engineers to invent and implement innovative approaches to get energy-efficient building designs [5], [6].

In addition to the significance of building design based on optimal energy consumption, the comfort of occupants is another essential issue in building design [7], [8]. Thermal comfort is a state of mind that demonstrates satisfaction with the thermal conditions of the environment [9], [10]. Among the well-known thermal comfort models, the predicted mean vote (PMV) and predicted percentage of dissatisfied (PPD) models are the most widely used [11], [12]. Fanger [13] initially expressed PMV and PPD models. The PMV model prognosticates the mean value of the votes of a large group of persons on the seven-point thermal sensation scale (+3 for hot, +2 for warm, +1 for slightly warm, 0 for neutral, -1 for slightly cool, -2 for cool, and -3 for cold). In addition, the PPD model establishes a quantitative prediction of the percentage of thermally dissatisfied people determined by PMV. The PPD model is based on the assumption that even when the thermal conditions are optimal for a majority, there will always be a percentage of people who feel thermal discomfort. The relationship between PMV and PPD is non-linear and has been empirically determined through extensive human subject studies. The PPD gives an estimate of the percentage of people who are likely to feel too warm or too cold in a given environment, not accounting for those who are neutral or satisfied. As per ASHRAE 55 [11], the admissible thermal environment for general comfort is recommended as PPD < 10% or -0.5 < PMV < +0.5. As the state of thermal comfort is often controlled using an air conditioning system, maintaining the standard of thermal comfort for

building occupants is one of the important goals of HVAC design engineers.

Energy efficiency in buildings will be acceptable when the thermal comfort of the occupants is also prepared. In this regard, to acquire an optimal building design, the energy-comfort criteria shall be taken into consideration in the design phases of the building, concomitantly.

As the decision-making process for adoption of the design specifications of buildings is made in the early stages of design and the building projects are complex multivariate problems, the building engineers and decision-makers encounter many feasible combinations for the configuration of building specifications [14], [15]. If the design principles are not paid attention to in the early stages, it may cause the wrong choice of building materials and equipment, and as a result, a building with low performance will be obtained. Accordingly, to get a building with the highest performance, the adoption of the best design parameters shall be carefully carried out.

Sensitivity analysis (SA) is a crucial step in the design and assessment of buildings, aiming to identify how variations in input parameters influence the output of a model. This understanding can guide the optimization of building performance, from energy efficiency to cost-effectiveness. To peruse and prognosticate the building performance, building designers mostly employ Building Energy Modeling Tools (BEMTs) including EnergyPlus, TRACE, Carrier HAP, DesignBuilder, eQUEST, and TRNSYS [16]-[19]. BEMTs take as input building specifications including geometry, orientation, construction materials, lighting, HVAC, refrigeration, water heating, renewable generation system configurations, component efficiencies, control strategies, schedules for occupancy, plug-loads, thermostat settings, information of weather, etc.; and prepare users with key indicators such as thermal loads, energy costs, temperature trends, thermal comfort indicators, air pollutants, ecological impact, etc. [20], [21].

BEMTs generally run the model of buildings scenario-by-scenario, which is an extremely time-consuming process and impractical to calculate all possible scenarios [22]. Coupling BEMTs with SA algorithms is a powerful approach that drives smarter, more efficient, and resilient building designs. It leverages the power of data and analytics to ensure that every decision made in the design, construction, and operation of buildings is informed, strategic, and geared towards sustainability and efficiency. This method leverages the strengths of both simulation and SA to explore and understand the impact of various parameters on building performance, without the need to manually simulate each possible scenario. Integrating BEMTs with SA algorithms offers a comprehensive approach to understanding and optimizing building performance. This integration not only enhances the predictive accuracy of energy models but also provides valuable insights for decision-making in the design and operation of buildings [23], [24]. There are many methods for SA of the systems, which are generally classified into two main categories, which include local sensitivity analysis (LSA) and global sensitivity analysis (GSA) [25], [26]. The LSA evaluates the local influence of changes in inputs on the system response [27]. The one-parameter-at-a-time (OPAT) analysis is one of the well-known LSA, in which the influence of one parameter on the outputs is apprised at a time, while other parameters of the system are kept constant at their nominal (central or baseline) values. Then, this process is repeated for other parameters similarly [28], [29]. In this regard, the SA index is measured by observing the changes in the outputs because of the single parameter changes within their specific range. Although the OPAT is easy to implement and efficient in terms of computational time, the simultaneous influence and interactions of all the inputs on outputs are not considered. As a result, it may provide inaccurate and confusing results regarding the prioritization of design parameters as per the degree of influence on the system, especially for non-linear and complex models such as building systems. On the other hand, GSA is a method in which all the input parameters are changed in their specific range concomitantly and the system sensitivity is appraised [30]. Consequently, GSA takes into account the interaction and mutual influence of the inputs on each other and demonstrates the system sensitivity to each input more accurately contrasted to LSA [31]. However, the calculation time in the GSA methods is much more than that of the LSA ones, especially for complex models with a large number of inputs [26]. Many methods have been introduced for the GSA in buildings so far including regression-based, Morris, variance-based, and metamodeling-based methods [32]. Among them, the variance-based has gained more popularity [33]-[35]. Sobol's method [36] is one of the well-known and most common variance-based GSA methods that are very practical and suitable for complex non-linear models [37]. Sobol's method considers complex and nonlinear interactions of inputs and uses more complicated sampling models to calculate the sensitivity indicators [38], [39]. In the past decade, because of the very valuable information that SA provides in the initial stages of building design, the attention of many researchers and decision-makers has been focused on the field of SA of building performance. Pang et al. [40] reviewed the application of SA in the building performance analysis (BPA) and summarized the major information

concerning the SA implementation in BPA. Shen et al. [41] performed scaled Morris-based SA of building energy-structure performance based on Python to connect with EnergyPlus and Abaqus. Similarly, Maučec et al. [42] performed Morris-based SA of a prefabricated timber building using SimLab and jEPlus tools. In addition, Sproul et al. [43] use TRNSYS to perform an LSA to clarify the correlation between building energy use and thermal comfort. Similarly, Huo et al. [44] performed regression-based SA for cooling demand and shading performance of nearly zero-energy buildings in China using SimLab. Besides, Goffart et al. [45] performed a comparative analysis of the random balance design Fourier amplitude sensitivity test (RBD-FAST) and the Morris screening using the Python sensitivity analysis library (SALib). They showed the EASI RBD-FAST is more powerful and easy to implement compared to Morris screening for building performance simulations. Additionally, Chambers et al. [46] carried out Saltelli sampling and Sobol SA for a geospatial model of cost-optimal heat electrification in buildings in Switzerland through SALib. Yip et al. [47] analyzed the effects of courtyards, passive and active design performance, and building-integrated photovoltaic and thermal (BIPV/T) integration on total building energy use in net zero energy buildings via TRNSYS, Python, and modeFRONTIER multidisciplinary design optimization platform. In another research, Zeferina et al. [48] used Morris and Sobol indices techniques to perform the SA of the cooling needs of an office building through jEplus. Naji et al. [49] performed the regression-based SA on energy performance, and thermal and visual discomfort of a prefabricated house in Australia using TRNSYS, jEPlus, and SimLab. In a similar study, Delgarm et al. [5] performed the variance-based GSA on the energy performance of a building using EnergyPlus, jEPlus, and MatLab. Bozzhigitov et al. [50] performed an SA of building energy performance to the selection of phase change materials (PCM) melting temperature in temperate oceanic climate using Design. Zhu et al. [51] performed the regression-based SA on building thermal loads for energy planning via EnergyPlus and R statistical computing and graphics software. Moreover, Zhang et al. [52] performed an SA for determining key parameters of net-zero energy buildings to optimize grid interaction using TRNSYS and MATLAB. Mukkavaara et al. [53] performed an SA considering the embodied and operational energy trade-off to minimize the energy use of the building's life cycle through SALib and EnergyPlus.

The background expresses that although several investigations have been carried out on the SA of building performance, most of them are focused on the LSA because of ease of use and low computing time. Moreover, building designers have either often used the existing SA software such as jEPlus, SimLab, SALib, modeFRONTIER, or manually made several runs from BEMTs and evaluated the outputs, which has many limitations. The adoption of the type and number of inputs to solve mixed-integer programming (MIP) problems concomitantly, the type and number of outputs, the method of SA as per the type of inputs and outputs, boundary conditions, and constraints are among the most important disadvantages and limitations of existing SA software. In addition to the fact that the existing SA software is developed based on different programming languages and needs to be coupled with the simulation engines, consequently, the computation time will be very long. In this regard, studies have suffered from a large amount of time spent on the SA process. Adding that, because of the complexity and difficulty of programming development, very few research have been focused on the numerical development of SBSA of building systems.

The current study introduces a new effective and efficient approach for the SBSA of building systems that not only helps building engineers to prognosticate and monitor the behavior of the building performance with respect to the variations in design parameters but also causes an increase in building productivity because of the accurate adoptions at the conceptual design phase. For this purpose, in a new idea, EnergyPlus is directly integrated with LSA and GSA algorithms through the C++ programming language. The developed method never depends on the type of design. It only deals with the (.txt) file. Thus, the proposed method can work for any model designed by EnergyPlus including smart buildings, zero energy buildings (ZEB), greenhouses, schools, and so on in any climate condition without difficulty. In this regard, a dwelling house located in Bushehr (Iran) with a hot semi-arid climate is used as a case study to examine the sufficiency of the proposed approach. The building rotation, window-to-wall ratio, depth of shading device, cooling and heating setpoint VAV system, the solar absorptance of the building interior walls and exterior walls, the thickness of building wall, solar and visible transmittance of window glass, the thickness of window glass, and thickness of gas in the window are selected as inputs. Further, the influences of inputs are fully scrutinized on the building energy loads and thermal comfort of occupants through OPAT and Sobol's analyses. In the OPAT approach, an innovative index is introduced to determine the sensitivity of outputs-to-inputs. To the best of the authors' knowledge, no similar article was found that deals with preparing a practical approach for SBSA of building performance through direct coupling of high-level object-oriented programming language with EnergyPlus to add its features and capabilities to EnergyPlus so as

to straightly perform SA without the use of other plugins and third parties. Because of the high importance of SBSA of efficacy-comfort criteria in the buildings, the background shows a lot of weakness, and therefore, studying them is not adequate and seems essential.

2. Methodology

2.1 *LSA approach*

In general, derivative-based LSA methods are based on the derivative of the outputs on the inputs. In this regard, the sensitivity index (SI) of the system due to the ith input (X_i) is expressed as [39], [54]:

$$\mathrm{SI}_i = \left.\frac{\partial Y}{\partial X_i}\right|_{X_0} \tag{1}$$

Here, Y and X_0 respectively signify the system output and nominal value. Derivative-based approaches are just enlightening at the nominal point because it does not search the rest of the input space. In addition, OPAT is in the LSA class and is highly suitable when $Y(X_i)$ is not available and the system behaves as a black box function. As per the OPAT technique, one of the inputs is changed in the entire permissible range one at a time and the values of the outputs are measured, while the other inputs are fixed in their nominal values. Since the OPAT provides a graph of the output versus the input changes, therefore, the authors introduced an indicator called Dispersion Index (DI) to define the sensitivity of outputs to each input (DI_i). DI is the ratio of the standard deviation of outputs (σ) to the average of outputs ($\bar{Y}$), calculated as:

$$\mathrm{DI}_i = \frac{\sigma}{\bar{Y}} \times 100 \tag{2}$$

The larger the DI, the greater the dispersion of the output, and therefore the input has a greater impact on the output. In other words, output is more sensitive to input.

2.2 *GSA approach*

Instead of evaluating the results of input changes on the system behavior through LSA at a time, the GSA evaluates the results of changing all possible inputs at the same time by considering the interactions of input variations concomitantly and reveals the relative contributions to the variability in the system output. In this paper, Sobol's analysis is employed to classify the inputs according to their importance and contribution to the outputs. Imagine that the function $Y = f(X)$ determines the system behavior as per its inputs ($X = [x_1, x_2, \ldots, x_m]$). In this respect, the algorithm of Sobol's analysis is implemented in three main steps as follows [39], [54]:

Step 1:
Decompose the total variance of the function $Y = f(X)$ with m inputs into conditional variances.

$$V(Y) = \sum_i^m D_i + \sum_i^m \sum_{j>i}^m D_{ij} + \ldots + D_{1,2,3,\ldots,m} \tag{3}$$

In the above equation, $V(Y)$ is the total variance of function Y, D_i is the first order influence for each x_i, and D_{ij} to $D_{1,2,3,\ldots,m}$ are the influences of inputs interaction, calculated as follows:

$$D_i = V\left[E_{X_{-i}}\left(Y|X_i\right)\right] \tag{4}$$

$$D_{ij} = V\left[E_{X_{-i}}\left(Y|X_i, X_j\right) - V_i - V_j\right] \tag{5}$$

$$D_{ijk} = V\left[E_{X_{-i}}\left(Y|X_i, X_j, X_k\right) - V_i - V_j - V_k\right] \tag{6}$$

and so on. Here, E and V represent the expected value and the variance, respectively. Moreover, $E(Y|X_i)$ is the conditional expectation. The term $V[E(Y|X_i)]$ is called the main influence of X_i on Y, and $E[V(Y|X_{-i})]$ is the residual. Additionally, X_{-i} signifies all inputs except for X_i. Accordingly, $V[E_{X_{-i}}(Y|X_i)]$ is the expected reduction in output variance and $E_{X_{-i}}[V(Y|X_{-i})]$ is the expected residual output variance that is obtained provided that X_i is fixed at the nominal value.

Step 2:

Determine the values of $V(Y)$, $V[E_{X_{-i}}(Y|X_i)]$, and $E_{X_{-i}}[V(Y|X_{-i})]$ through the quasi-Monte Carlo estimators. To do this, two independent sampling matrices A and B are made by Sobol quasi-random sequences with M rows and m columns. M and m are respectively the sample size of Sobol quasi-random sequences and the number of inputs. Matrix C_i is made from matrices A and B in such a way that all the columns of matrix A are placed in matrix C, but only the ith column of matrix B is placed in matrix C. In this regard, the system outputs are $Y_A^{(m)}$, $Y_B^{(m)}$, and $Y_C^{(m)}$ with the values of matrices A, B, and C as inputs. Accordingly, $V(Y)$, $V[E_{X_{-i}}(Y|X_i)]$, and $E_{X_{-i}}[V(Y|X_{-i})]$ are determined as [55]:

$$V(Y) = \frac{1}{M}\sum_{j=1}^{M}\left[Y_A^{(m)}\right]^2 - \left[\frac{1}{M}\sum_{j=1}^{N}\left[Y_A^{(m)}\right]\right]^2 \tag{7}$$

$$V\left[E_{X_{-i}}\left(Y|X_i\right)\right] = V(Y) - \frac{1}{2M}\sum_{j=1}^{M}\left[Y_B^{(m)} - Y_{C_i}^{(m)}\right]^2 \tag{8}$$

$$E_{X_{-i}}\left[V\left(Y|X_{-i}\right)\right] = \frac{1}{2M}\sum_{m=1}^{M}\left[Y_A^{(m)} - Y_{C_i}^{(m)}\right]^2 \tag{9}$$

In the present paper, M of 2,000 and m of 12 columns are adopted to compute the above formulas.

Step 3:

Calculate the total-order SI (S_{Ti}):

$$S_{Ti} = \frac{E_{X_{-i}}\left[V\left(Y|X_{-i}\right)\right]}{V(Y)} \tag{10}$$

The larger the S_{Ti}, the more sensitive the output is to the input. The S_{Ti} index expresses the whole impact of an input on the system outputs considering all of its interactions with other inputs and discloses the expected portion of variance that remains if uncertainty is removed in all inputs but X_i. The S_{Ti} is the overall best SI of outputs-to-inputs since it covers the full individual and interactive influences of system inputs, concomitantly.

2.3 Integration framework

Figure 1 demonstrates the proposed integration framework for SBSA of building performance via coupling EnergyPlus with algorithms of OPAT and Sobol's analyses. EnergyPlus is a whole-building energy simulation software developed by the U.S. Department of Energy's (DOE) Building Technologies Office (BTO) and was first released in 2001 and an updated version 23.1.0 was released in 2023 [56]. EnergyPlus supports for calculating the building energy efficiency of heating, cooling, ventilation, lighting, and other energy flows, and consists of many creative and useful capabilities in simulation including multi-zone airflow, thermal and visual comfort, solar-based systems, etc. As demonstrated in Figure 1, the inputs of the proposed SBSA approach are the weather data, building design parameters, output variables, input variables whose influences on the output variables are to be studied, and the range of input variables (constraints). As EnergyPlus only relies on input/output data that reads input and writes output to text files, through a new initiative, coupling functions (command lines) were developed via C++ programming language to launch EnergyPlus and make it run based on the randomly produced inputs $[(X_i)]$ as per the Sobol quasi-random sequences, weather data, and basic model of the building. After that, the EnergyPlus simulation outputs $([F(X_i)])$ are assembled for post-processing. The algorithm of OPAT and Sobol's analyses are programmed through C++ programming language to analyze $[F(X_i)]$. The OPAT analysis yields the trend of the outputs versus input changes and DI of each output to input, regardless of the interaction of the other inputs. In addition, Sobol's analysis yields the total-order SI (S_{Ti}) of each output to input considering the interactions of inputs changes concomitantly. Consequently, the presented paper introduces an innovation, in which adding SA to EnergyPlus is directly accomplished without the use of other plugins and third parties that dramatically increase the speed of computation. While many studies have investigated the SA of building performance, authors have not come across a similar paper that deals with preparing a practical and structured approach for SBSA of building performance by using direct coupling of a high-level programming language with building simulation software. In this regard, through a new initiative, the LSA and GSA are directly combined with EnergyPlus via C++ as an object-oriented programming language, and accordingly, the features of C++ are added to EnergyPlus. As a result, any kind of SA algorithm, any number and type of inputs, any number of outputs, and any constraints can be utilized through the introduced approach. In addition, as the proposed method only deals with the (.txt) file, thus, it can work for any model designed by EnergyPlus in any climate condition without limitation.
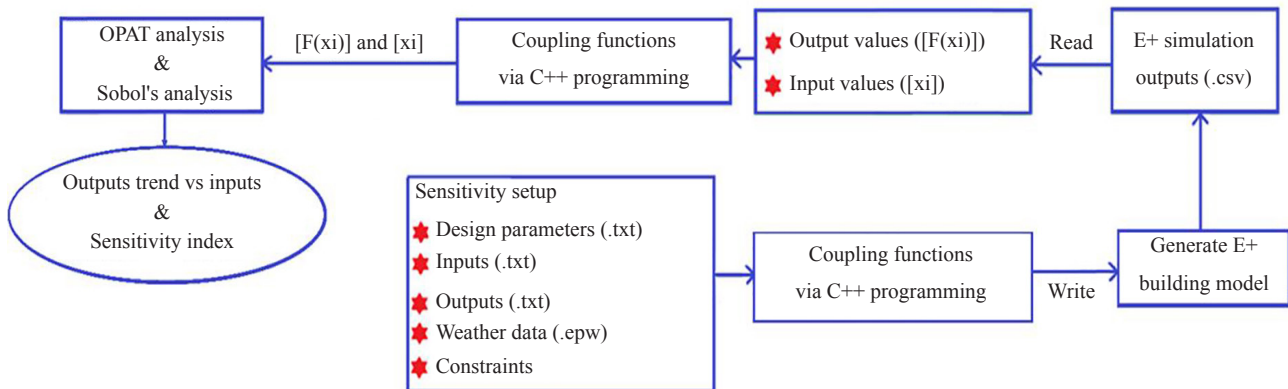

Figure 1. Integration framework

2.4 Case study

2.4.1 Building characteristics

The developed SBSA approach is implemented on a dwelling house located in the hot semi-arid climate of Iran to examine its capabilities and potential. Figure 2 demonstrates the schematic view of the basic model of the building

under investigation, which is created in SketchUp 3D design software [57]. The building is a five-person dwelling house with a height of 3 m, length of 10 m, and width of 10 m. The initial building facade (BF) is to the north, and the direction of building rotation is counterclockwise. The building has an east-facing fixed double-glazed window (3 mm clear glazing with an argon 6 mm gas gap) with a width of 1.5 m and a length of 4 m (WWR of 20%), and a wooden door on the eastern side with a height of 1.5 m and a width of 2 m. The window has a flat shading surface with a length of 4 m and a depth of 1 m, but no curtains are prepared for it. Further, the height above the window, as well as the left and right extension from the window of the flat shading surface remain zero, while the tilt angle from the window is kept at 90°. Table 1 demonstrates the specifications of the materials employed for the building under investigation.
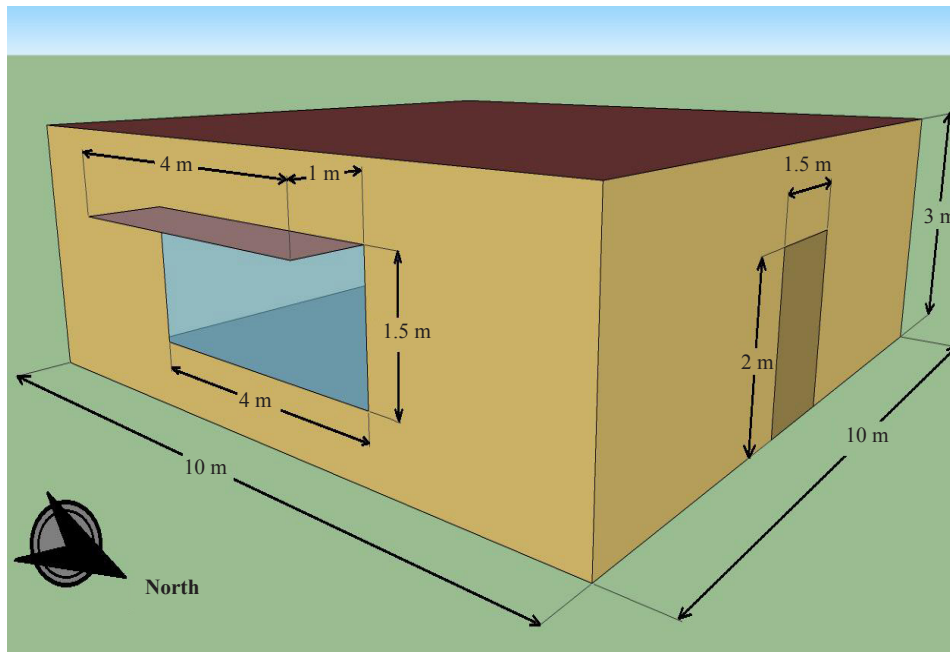

Figure 2. SketchUp 3D model of the basic building model under investigation

A 500 Watts fluorescent artificial lighting system is used in working hours whose power can be dimmed by a daylight sensor with an activation threshold of 500 lux to control the room luminance automatically when the natural light of the sun is not sufficient. The sensor is located in the middle of the room and at 1 m above the floor. In addition, a variable air volume (VAV) system with an outdoor airflow rate of 9.5 *l/s* per person is installed for the building whose capacity is automatically perused as per the warmest and the coldest days of the year. As per the United States Environmental Protection Agency (EPA) [58], the optimal cooling and heating setpoint temperatures to balance energy saving and comfort, and provide appropriate thermal comfort to 80% of building occupants is respectively close to 24.5 °C and 21 °C. Accordingly, the cooling and heating setpoints of VAV were respectively set at 24.5 °C and 21 °C for the zone thermostat control. The illuminance threshold of 500 lux was set as recommended by EN 12464-1 for office space [59]. Moreover, the schedules for clothing, lighting, occupancy, air velocity, and infiltration are arranged as per the EnergyPlus data set [56].

Table 1. Specifications of the building envelope under investigation

Envelope	Specification		Value
Wall	Exterior layer (brick)	Conductivity (W/mK)	0.89
		Thickness (m)	0.1016
		Specific heat (J/kgK)	790
		Density (kg/m^3)	1,920
	Interior layer (Wood shingles)	Conductivity (W/mK)	0.04
		Thickness (m)	0.0064
		Specific heat (J/kgK)	1,300
		Density (kg/m^3)	592
Floor	Exterior layer (heavyweight concrete)	Conductivity (W/mK)	1.95
		Thickness (m)	0.3048
		Specific heat (J/kgK)	900
		Density (kg/m^3)	2,240
	Interior layer (Terrazzo)	Conductivity (W/mK)	1.8
		Thickness (m)	0.0254
		Specific heat (J/kgK)	790
		Density (kg/m^3)	2,560
Roof	Exterior layer (lightweight concrete block)	Conductivity (W/mK)	0.49
		Thickness (m)	0.1524
		Specific heat (J/kgK)	800
		Density (kg/m^3)	512
	Middle layer (gypsum)	Conductivity (W/mK)	0.16
		Thickness (m)	0.0159
		Specific heat (J/kgK)	1,090
		Density (kg/m^3)	800
	Interior layer (Wood shingles)	Conductivity (W/mK)	0.04
		Thickness (m)	0.0064
		Specific heat (J/kgK)	1,300
		Density (kg/m^3)	592

Table 1. (cont.)

Envelope	Specification		Value
Door	Exterior layer (Wood)	Conductivity (W/mK)	0.15
		Thickness (m)	0.0127
		Specific heat (J/kgK)	1,630
		Density (kg/m^3)	608
window	Double 2.5 mm clear glazing	Solar transmittance	0.85
		Visible transmittance	0.901
		Conductivity (W/mK)	0.9
		Thickness (m)	0.0025

2.4.2 *Climate region*

Iran is situated in Western Asia with an area of about 1.65 million km^2 along the coastline of the Sea of Oman and the Persian Gulf to the south [60], [61]. Iran has a hot-dry climate characterized by long hot-dry summers and short cool winters [62]. Bushehr is a port city situated on the Persian Gulf coast in southern Iran with a hot semi-arid climate whose temperature alters from 12 °C to 37 °C and rarely reaches below 9 °C or above 39 °C during the year [63], [64]. It has a latitude of 28.9036N and a longitude of 50.8208E, respectively. The annual heating degree-days (HDDs) and cooling degree-days (CDDs), with a base temperature of 18.3 °C, are respectively 217 and 2,847 [65], [66]. In this research, Bushehr is adopted as a representative city for the studied climate, whose weather information in epw format prepared by the DOE BTO [56] is employed for the EnergyPlus simulations.

2.4.3 *Inputs, outputs, and constraints*

In this paper, four output variables including annual heating energy use (AHC), annual cooling energy use (ACC), annual lighting energy use (ALC), and predicted percentage of dissatisfied (PPD) index as a measure of the occupant thermal comfort level were adopted. All four outputs are calculated directly by the EnergyPlus. In addition, the building rotation (BR) from the north axis, window-to-wall ratio (WWR), depth of shading device (DSH), cooling and heating setpoints (CSPT and HSPT), solar absorptance of the building walls including interior walls (SA_{IN_W}) and exterior walls (SA_{Ex_W}), thickness of building wall (Th$_{Ex\_W}$), solar transmittance of window glass (ST$_{win}$), visible transmittance of window glass (VT$_{win}$), thickness of window glass (Th$_{win}$), thickness of gas in window (Th$_{gas\text{-}win}$) with iteration step of 400 for each variable were adopted as inputs. The characteristics of the input variables are detailed in Table 2.

Table 2. Characteristics of the input variables

Item	Input	Unit	Initial value	Range	Type
x_1	BR	°	0	[0, 360)	Continues
x_2	WWR	-	0.2	(0, 1)	Continues
x_3	DSH	m	1	(0, 1.5]	Continues
x_4	CSPT	°C	24.5	(22, 30]	Continues
x_5	HSPT	°C	21	[13, 22]	Continues
x_6	SA_{IN_W}	-	0.505	[0, 1]	Continues
x_7	SA_{Ex_W}	-	0.311	[0, 1]	Continues
x_8	Th_{Ex_W}	m	0.1	[0.1, 0.4]	Continues
x_9	ST_{win}	-	0.837	[0, 1]	Continues
x_{10}	VT_{win}	-	0.898	[0, 1]	Continues
x_{11}	Th_{win}	mm	3	[1, 16]	Continues
x_{12}	$Th_{gas-win}$	mm	6	[1, 14]	Continues

4. Results and discussion

In this section, the results of the implementation of the introduced method on the building under study in Bushehr (Iran) with a hot semi-arid climate are presented. First, the OPAT analysis as the LSA is performed to determine the behavior of outputs versus inputs and find out how the outputs are affected due to input changes. In addition, the DI of each output to input is appraised, regardless of the interaction of the other inputs. Then, Sobol's analysis as the GSA is performed to quantify and prioritize the sensitivity of outputs-to-inputs.

4.1 *Results of OPAT analysis*

This part of the investigation explores the influence of BR, WWR, DSH, CSPT, HSPT, SA_{IN_W}, SA_{Ex_W}, Th_{Ex_W}, ST_{win}, VT_{win}, Th_{win}, $Th_{gas-win}$ on the AHC, ACC, ALC, and PPD employing the OPAT approach. To this end, one input is changed over its boundary one at a time and the other inputs are kept fixed at their nominal values (as given in Table 1 and Table 2) and the response of the outputs is measured.

4.1.1 *Influence of BR*

Figure 3 indicates the influence of BR on the AHC, ACC, ALC, and PPD. As observed, the lowest amount of AHC, ACC, ALC, and PPD was obtained at an angle of 90 (BF to the east), 272 (BF to the west), 128 (BF to the southwest), and 298 (BF to the northeast), respectively. Accordingly, the building system had a completely non-linear and complex behavior about the BR. Hence, a Pareto optimization is needed to find the optimum BR in such a way that both annual total energy consumption (ATC) and PPD criteria have their optimal values. Overall, the DI of AHC, ACC, ALC, and PPD were respectively 12%, 3%, 8%, and 1%, which means that the BR has the most influence on the AHC and the

least influence on the PPD, without considering the influence of other inputs. Without defining the DI index, it was not possible to understand the sensitivity of outputs to BR.
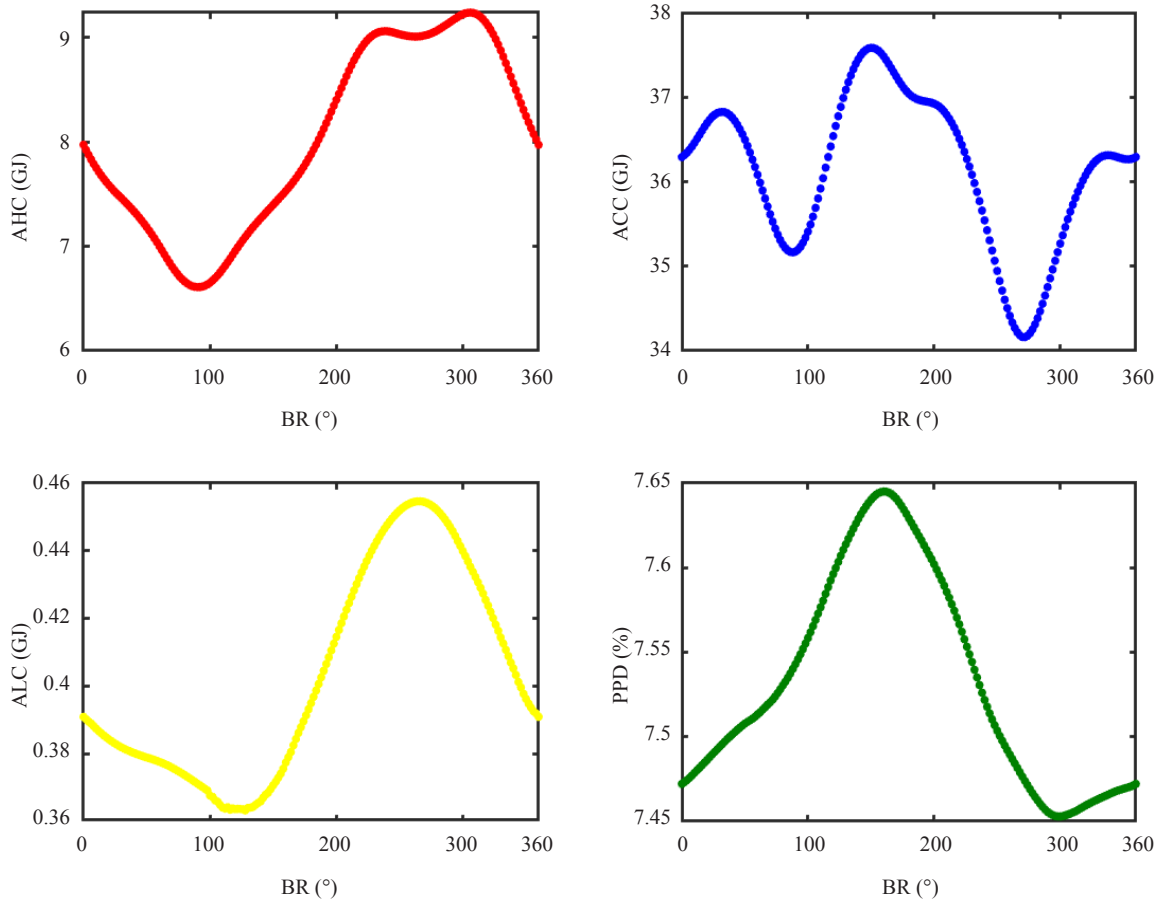

Figure 3. Influence of BR on the AHC, ACC, ALC, and PPD

4.1.2 *Influence of WWR*

Figure 4 indicates the influence of WWR on the AHC, ACC, ALC, and PPD. As observed, with the increase in WWR from 0% to 100%, the AHC and ALC decreased while ACC and PPD increased because of the increase in receiving lighting and heating energy from the outside environment into the building. Accordingly, a Pareto optimization is needed to find the optimum WWR in such a way that both ATC and PPD criteria have their optimal values. In addition, AHC and ACC changes were linear while PPD and ALC changes were exponentially contrasted to WWR changes. With the increase in window size, the annual cooling energy use increased compared to the initial model due to the excessive rise of the solar energy into the room model, which led to a decrease in the annual heating energy demand. Besides, the lighting energy demands decreased compared to the initial model because of the increment of the lighting energy from the outside into the building model. The DI of AHC, ACC, ALC, and PPD were respectively 27%, 18%, 28%, and 7%, which shows that the WWR has the most influence on the AHC and ALC and the least influence on the PPD.
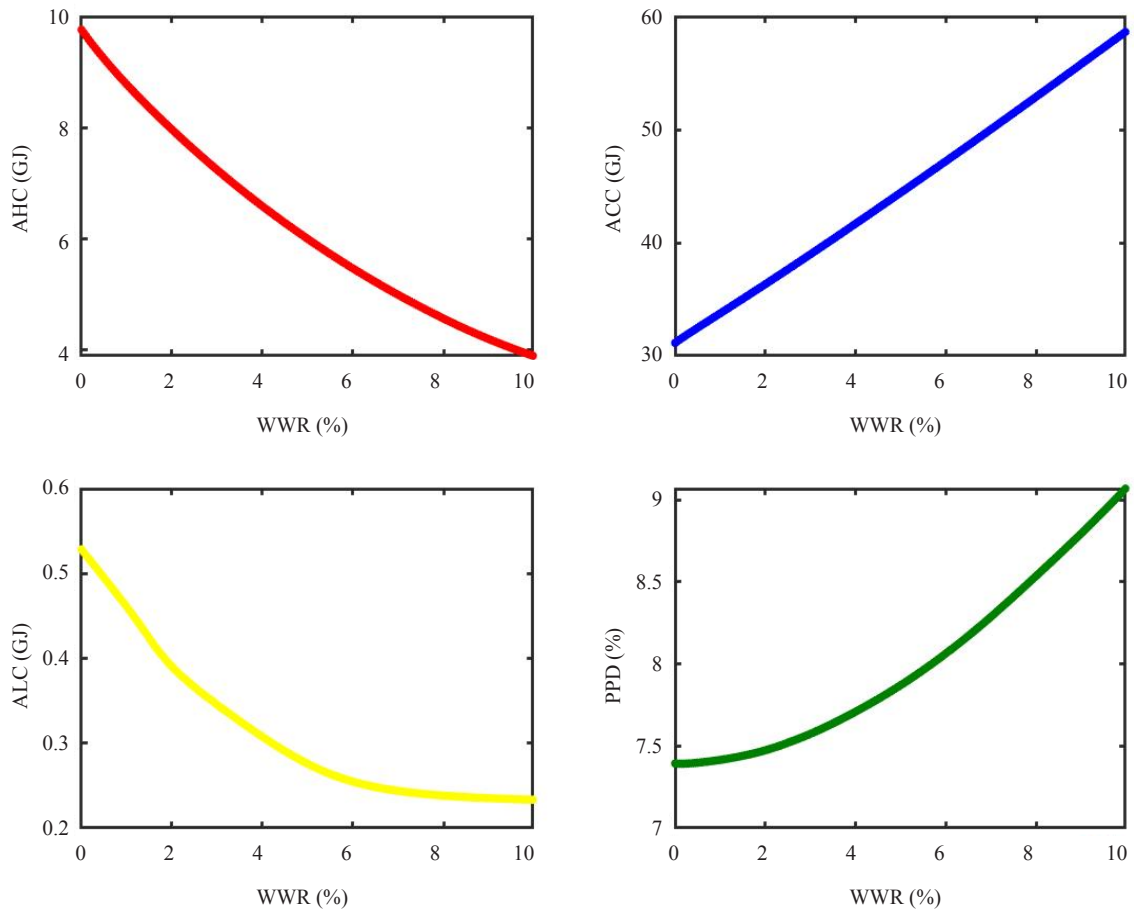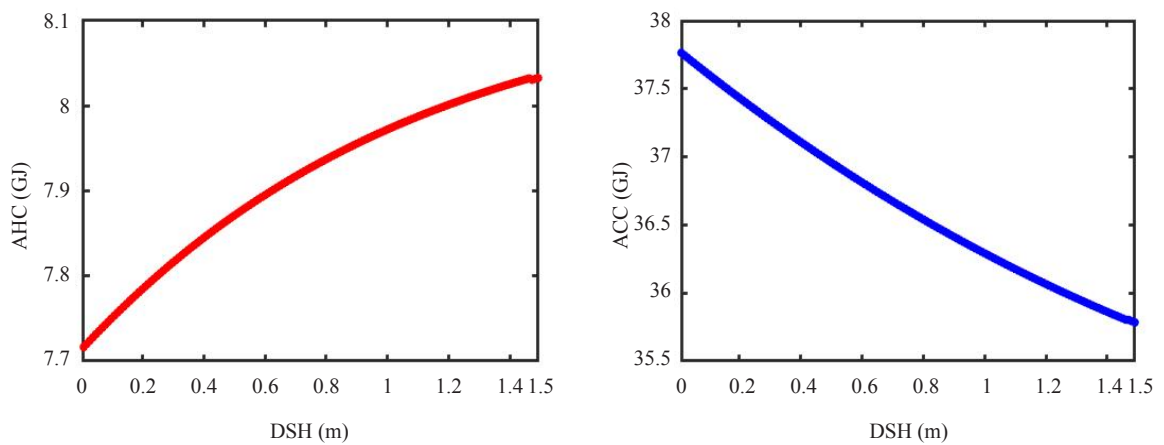
Figure 4. Influence of WWR on the AHC, ACC, ALC, and PPD
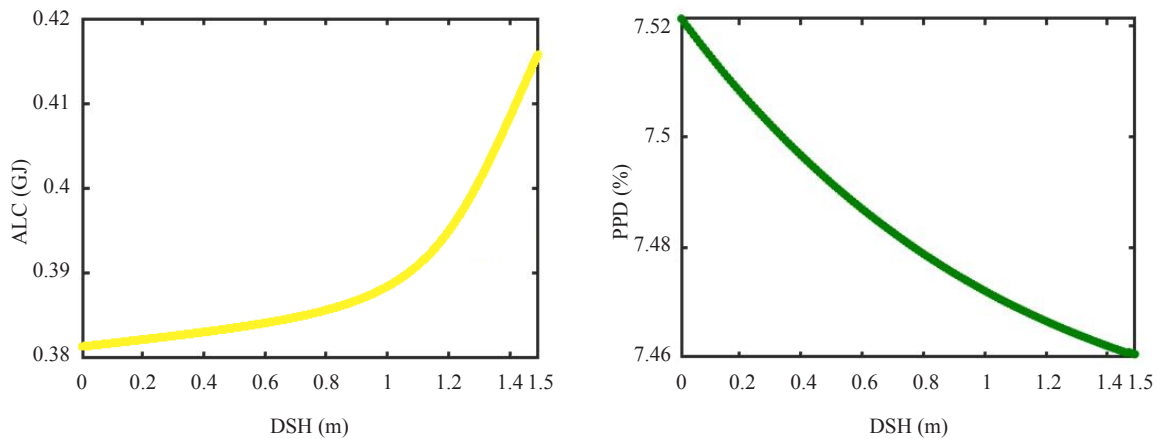
4.1.3 Influence of DSH

Figure 5. Influence of DSH on the AHC, ACC, ALC, and PPD

Figure 5 indicates the influence of DSH on the AHC, ACC, ALC, and PPD. As observed, with the increase in DSH from 0 m to 1.5 m, the AHC and ALC increased while PPD and ACC decreased because of the decrease in receiving lighting and heating energy from the outside environment into the building. With the increase in DSH, the annual cooling energy demand decreased. The annual heating and lighting increase because of the gradual decline of the solar energy entrance into the building model with the increase in DSH. Accordingly, a Pareto optimization is needed to find the optimum DSH in such a way that both ATC and PPD criteria have their optimal values. In addition, AHC, ACC, ALC, and PPD changes were almost exponentially contrasted to DSH changes. Hence, the DI of AHC, ACC, ALC, and PPD were respectively 2%, 2%, 2%, and 1%, which expresses that DSH has a small influence on AHC, ACC, ALC, and PPD.

4.1.4 *Influence of CSPT*

Figure 6 indicates the influence of CSPT on the AHC, ACC, ALC, and PPD. As observed, with the increase in CSPT from 22 °C to 33 °C, the AHC and ACC decreased while it did not affect the ALC, which shows the ALC is not dependent on CSPT. In addition, with the increase in CSPT, the PPD first decreased, but above the temperature of 24 °C, it sharply increased. The reason is that as the CSPT increases, the conditions of thermal comfort of occupants become favorable as per the Fanger model [13], but above the temperature of 24 °C because the VAV system does not start operating until it reaches the high value of CSPT, which leads to the feeling of high heat and discomfort in the occupants. Accordingly, despite the reduction of ATC due to the non-starting of the VAV system until it reaches the high CSPT, the thermal comfort conditions become unfavorable and the PPD deviates from the sweet spot. Additionally, the PPD trend versus CSPT is in accordance with the CSPT value recommended by the EPA [58]. Accordingly, a Pareto optimization is needed to find the optimum CSPT in such a way that both ATC and PPD criteria have their optimal values. Further, the ACC changes were almost linear while AHC and PPD changes were respectively exponential and parabolic in contrast to CSPT changes. Overall, the DI of AHC, ACC, ALC, and PPD were respectively 1%, 54%, 0%, and 64%, which means that the CSPT has the most influence on the PPD and ACC while has the least influence on the AHC and ALC.
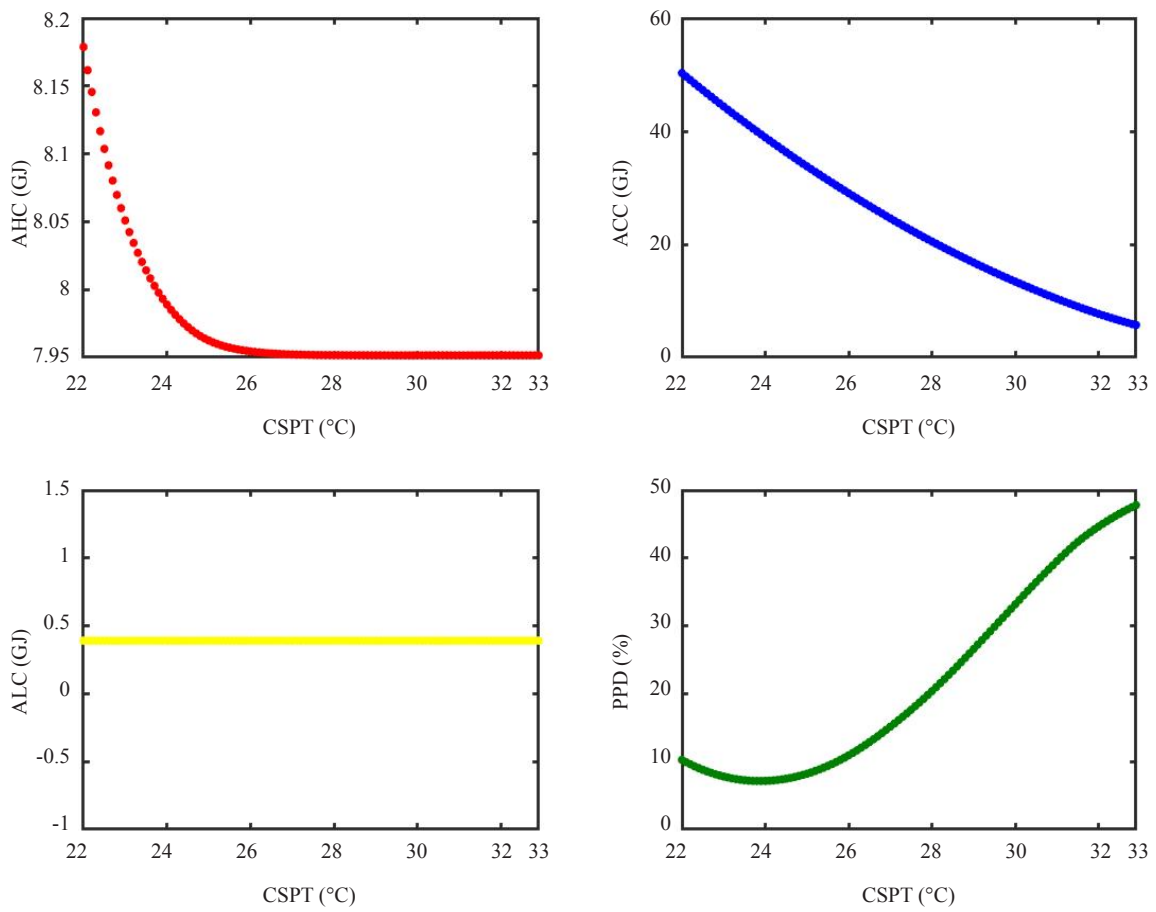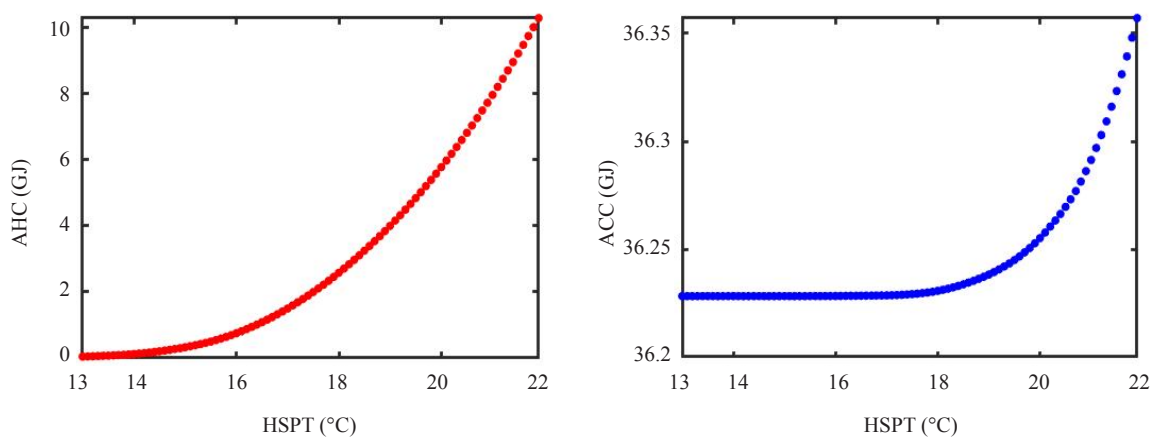
Figure 6. Influence of CSPT on the AHC, ACC, ALC, and PPD
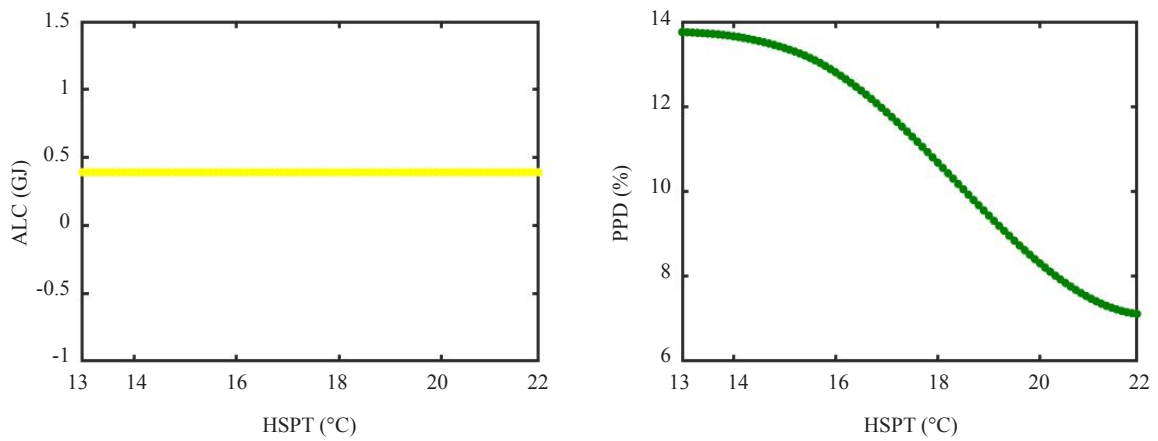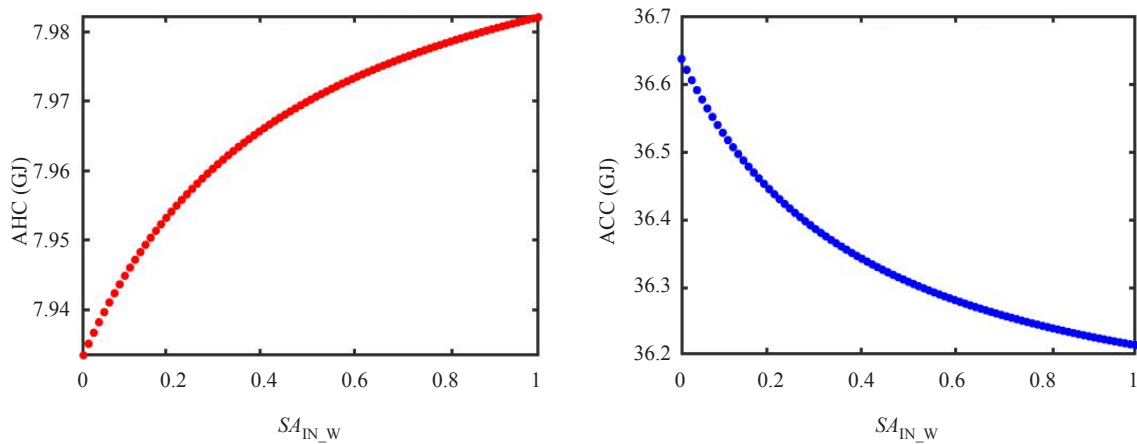
4.1.5 *Influence of HSPT*

Figure 7. Influence of HSPT on the AHC, ACC, ALC, and PPD

Figure 7 indicates the influence of HSPT on the AHC, ACC, ALC, and PPD. As observed, unlike the influence of CSPT on AHC and ACC, with the increase in HSPT from 13 °C to 22 °C, the AHC and ACC increased. However, similar to the influence of CSPT on ALC, the HSPT did not affect the ALC. In addition, with the increase in HSPT from very cold to moderate temperature, the PPD decreased as the thermal comfort conditions of occupants became favorable as per the Fanger model [13] and the PPD approached the sweet spot. Additionally, the PPD trend versus HSPT is in accordance with the HSPT value recommended by the EPA [58]. In addition, the AHC and ACC changes were exponential while PPD changes were parabolic in contrast to HSPT changes. Accordingly, a Pareto optimization is needed to find the optimum HSPT in such a way that both ATC and PPD criteria have their optimal values. Overall, the DI of AHC, ACC, ALC, and PPD were respectively 92%, 1%, 0%, and 22%, which indicates that HSPT has the most influence on the AHC and the least influence on the ACC and ALC.
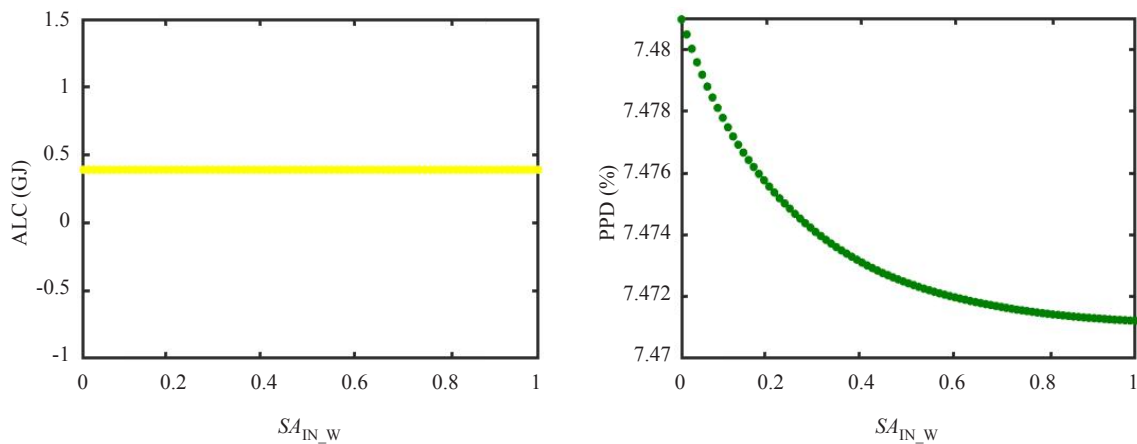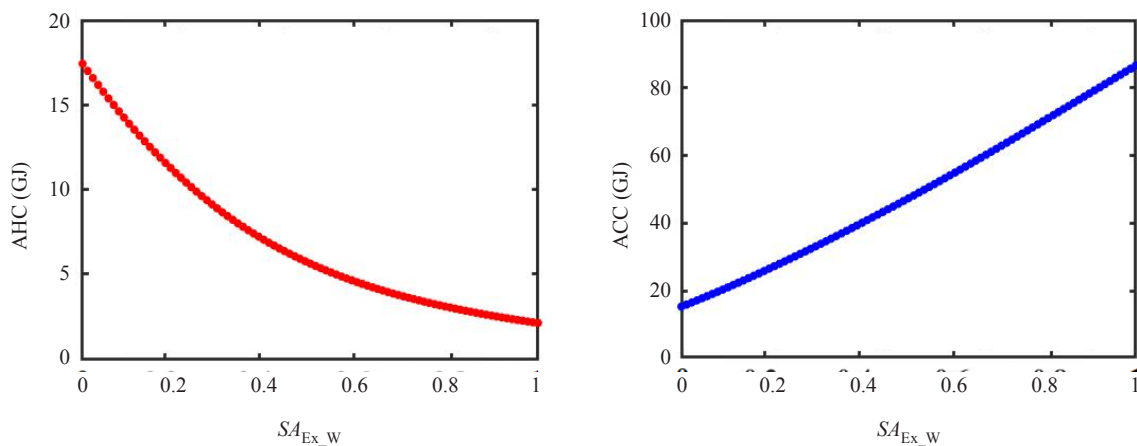
4.1.6 Influence of SA_{IN_W}

Figure 8. Influence of SA_{IN_W} on the AHC, ACC, ALC, and PPD

Figure 8 indicates the influence of SA_{IN_W} on the AHC, ACC, ALC, and PPD. As observed, with the increase in SA_{IN_W} from 0 to 1, the ACC and PPD decreased while the AHC increased. However, SA_{IN_W} did not affect the ALC. In other words, the darker the color of the interior wall, the lower the amount of ACC and PPD and the higher the amount of AHC. Accordingly, a Pareto optimization is needed to find the optimum SA_{IN_W} in such a way that both ATC and PPD criteria have their optimal values. Inner walls with appropriate solar absorptance can absorb heat during the day and release it at night, contributing to a more stable and comfortable indoor temperature. This effect is particularly beneficial in spaces that experience significant temperature fluctuations, helping to maintain a consistent thermal environment that aligns with human comfort levels. In addition, the AHC, ACC, and PPD changes were exponential in contrast to SA_{IN_W} changes. Overall, the DI of AHC, ACC, ALC, and PPD were respectively 1%, 1%, 0%, and 1%, which means that SA_{IN_W} has a small influence on AHC, ACC, ALC, and PPD.
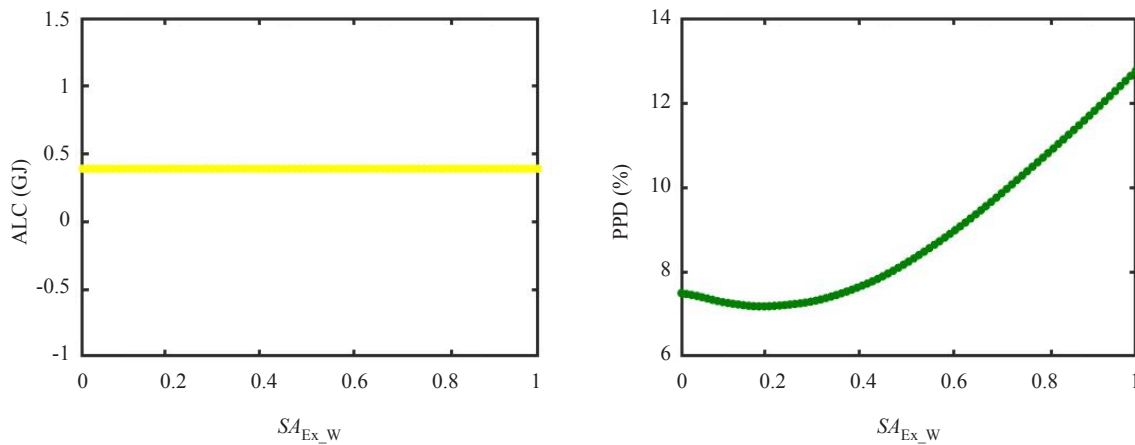
4.1.7 Influence of SA_{Ex_W}

Figure 9. Influence of SA_{Ex_W} on the AHC, ACC, ALC, and PPD

Figure 9 indicates the influence of SA_{Ex_W} on the AHC, ACC, ALC, and PPD. As observed, with the increase in SA_{Ex_W} from 0 to 1, the AHC decreased while ACC and PPD increased. However, SA_{Ex_W} did not affect the ALC. In other words, the darker the color of the exterior wall, the lower the amount of AHC and the higher the amount of ACC and PPD. Accordingly, a Pareto optimization is needed to find the optimum SA_{Ex_W} in such a way that both ATC and PPD criteria have their optimal values. The external walls with high solar absorptance absorb more solar energy, leading to increased heat gain within the building. This can significantly increase the cooling demand, leading to higher energy consumption by air conditioning systems. Conversely, walls with lower solar absorptance reflect more solar radiation, helping to reduce cooling loads and energy consumption. In addition, the AHC and PPD changes were respectively exponential and parabolic; however, ACC linearly changed contrasted to SA_{Ex_W} changes. Overall, the DI of AHC, ACC, ALC, and PPD were respectively 63%, 44%, 0%, and 20%, which means that SA_{Ex_W} has the most influence on the AHC and the least influence on the ALC.

4.1.8 Influence of Th_{Ex_W}

Figure 10 indicates the influence of Th_{Ex_W} on the AHC, ACC, ALC, and PPD. As observed, with the increase in Th_{Ex_W} from 0.1 m to 0.4 m, the AHC, ACC, and PPD decreased almost parabolically. However, Th_{Ex_W} did not affect the ALC. Enhanced Th_{Ex_W} significantly improves insulation properties, effectively reducing thermal bridging and heat transfer between the building's interior and the external environment. This reduction in heat transfer directly correlates with a decrease in annual cooling and heating energy demands, as less energy is required to maintain optimal indoor temperatures, irrespective of the external climatic conditions. Moreover, the increased thermal mass provided by thicker walls contributes to more stable indoor temperatures, mitigating the impact of daily and seasonal temperature fluctuations. This stability enhances occupant comfort by minimizing the variations in indoor thermal conditions, leading to environments that are naturally more consistent and comfortable. Consequently, optimizing the thickness of external walls presents a tangible strategy for achieving substantial energy savings while simultaneously enhancing the quality of indoor living spaces, making it a critical consideration for sustainable building design and construction. The strategic implementation of wall thickness adjustments, therefore, not only aligns with environmental sustainability goals but also significantly contributes to the health, well-being, and satisfaction of building occupants. As a result, a thicker wall provides extra insulation, making a home more energy-comfort efficient, comfortable, and soundproof, which is in agreement with the results obtained by Yu et al. [67]. However, thicker walls need more material, which adds costs and weight. In this regard, a cost-benefit analysis is needed for adopting the best Th_{Ex_W}. Overall, the DI of AHC, ACC, ALC, and PPD were respectively 10%, 6%, 0%, and 2%, which means that Th_{Ex_W} has the most influence on the AHC and the least influence on the ALC.
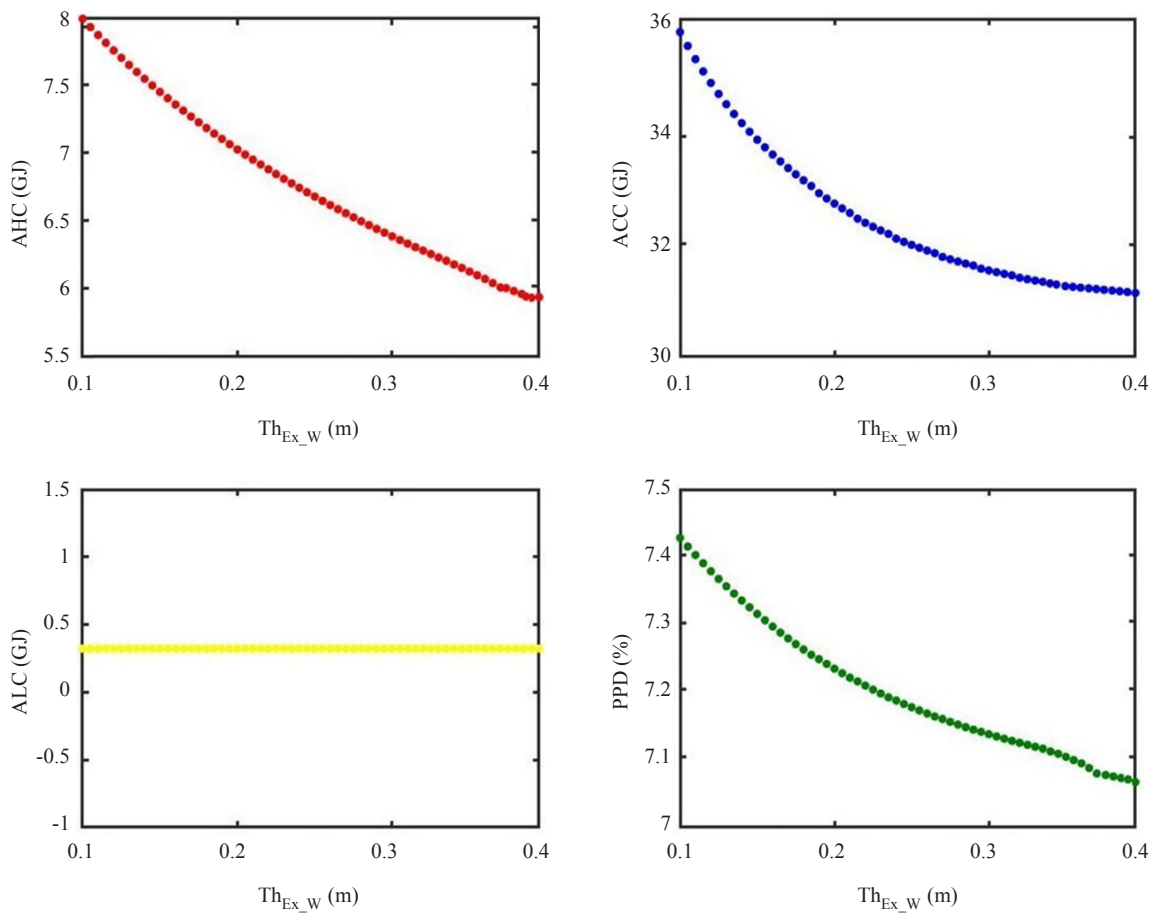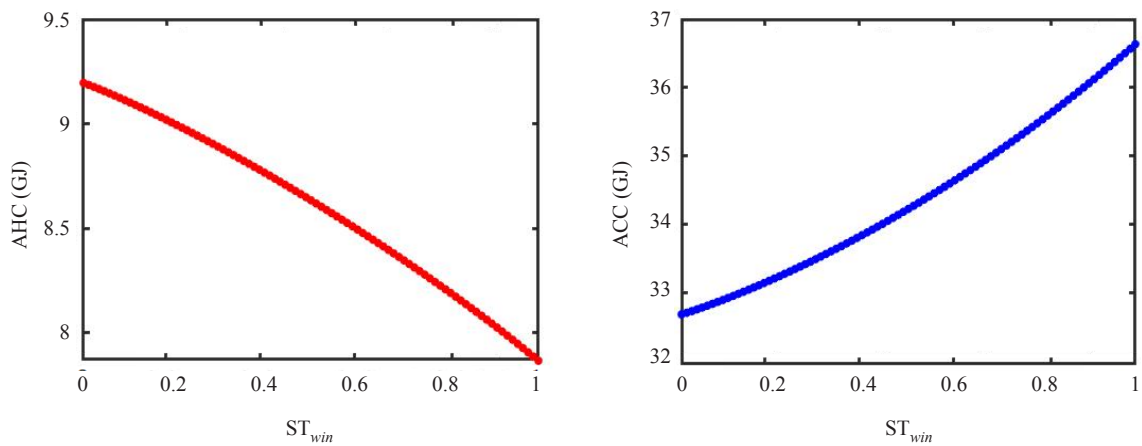
Figure 10. Influence of Th_{Ex_W} on the AHC, ACC, ALC, and PPD

4.1.9 Influence of ST_{win}

Figure 11. Influence of ST$_{win}$ on the AHC, ACC, ALC, and PPD

Figure 11 indicates the influence of ST$_{win}$ on the AHC, ACC, ALC, and PPD. As observed, with the increase in ST$_{win}$ from 0 to 1, the AHC decreased while the ACC and PPD increased because of the increase in solar heat entering the building through the window glass. However, ST$_{win}$ did not affect the ALC. High ST$_{win}$ allows for an abundance of solar heat energy, potentially elevating total cooling demands and decreasing total heating demands. Accordingly, a Pareto optimization is needed to find the optimum ST$_{win}$ in such a way that both ATC and PPD criteria have their optimal values. In addition, the AHC, ACC, and PPD changes were almost parabolic in contrast to ST$_{win}$ changes. Overall, the DI of AHC, ACC, ALC, and PPD were respectively 5%, 4%, 0%, and 1%, which means the ST$_{win}$ has the most influence on the AHC and ACC and the least influence on the ALC. However, it is observed that ST$_{win}$ has a small influence on AHC, ACC, ALC, and PPD.
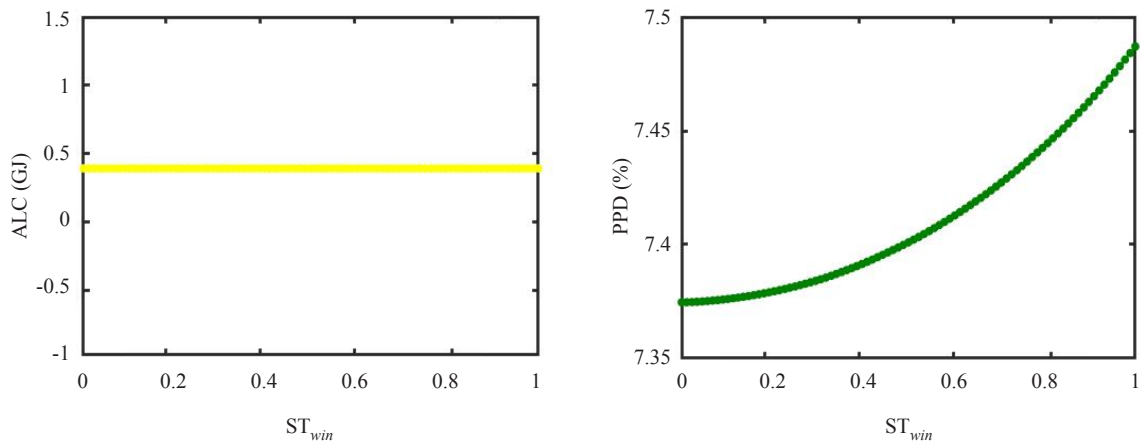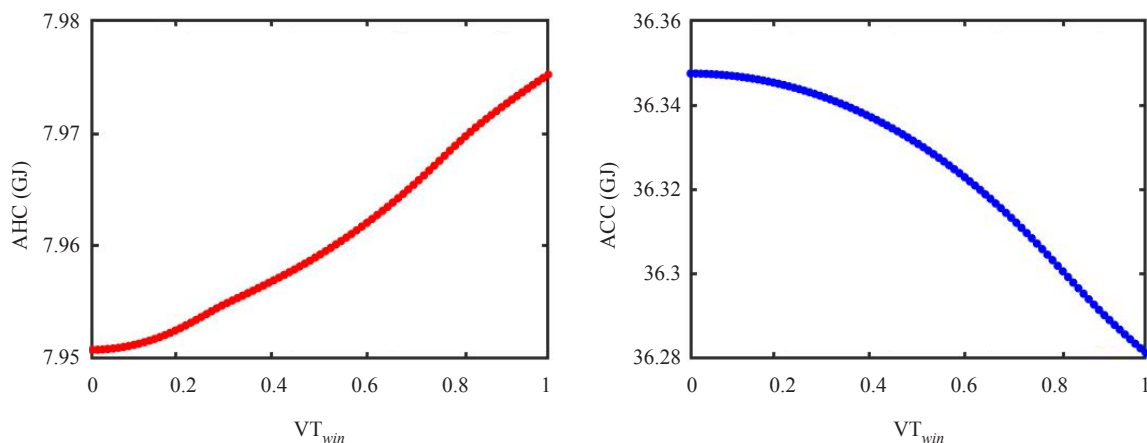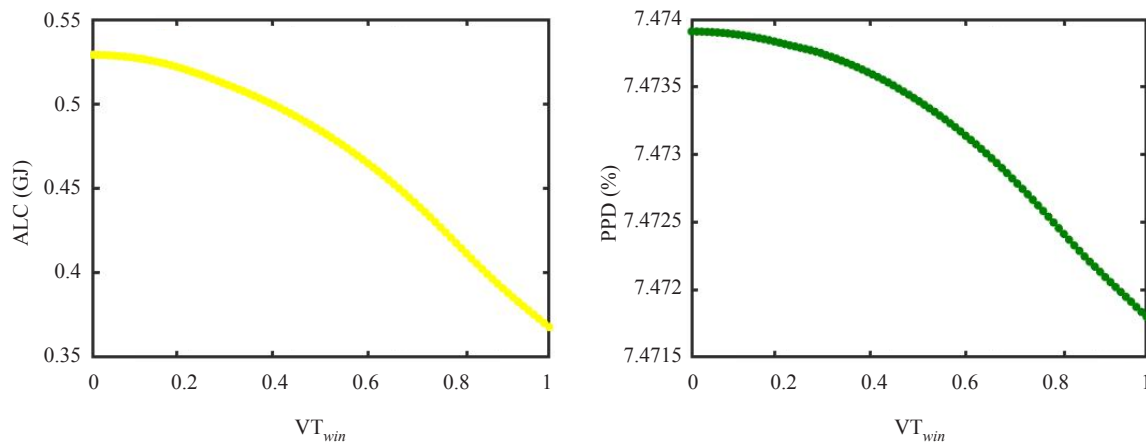
4.1.10 *Influence of VT$_{win}$*

Figure 12. Influence of VT_{win} on the AHC, ACC, ALC, and PPD

Figure 12 indicates the influence of VT_{win} on the AHC, ACC, ALC, and PPD. As observed, with the increase in VT_{win} from 0 to 1, the AHC increased a little while the ACC, ALC, and PPD almost parabolically decreased because of the increase in lighting energy entering the building through the window glass. High VT_{win} promotes the penetration of natural daylight, significantly enhancing interior brightness and reducing the reliance on artificial lighting. This increase in natural light has been linked to improved mood, increased productivity, and even better physical health for occupants. Accordingly, a Pareto optimization is needed to find the optimum VT_{win} in such a way that both ATC and PPD criteria have their optimal values. Overall, the DI of AHC, ACC, ALC, and PPD were respectively 1%, 1%, 11%, and 1%, which means that VT_{win} has the most influence on the ALC and the least influence on the AHC, ACC, and PPD.

4.1.11 *Influence of Th_{win}*

Figure 13 indicates the influence of Th_{win} on the AHC, ACC, ALC, and PPD. As observed, with the increase in Th_{win} from 1 mm to 15 mm, the AHC, ACC, and PPD linearly decreased a little. However, Th_{win} did not affect the ALC. High Th_{win} offers improved thermal insulation, reducing the conductive heat transfer from the hot exterior to the cooler interior. This enhancement in insulation can significantly decrease the building's cooling demands by limiting the amount of heat that enters, thereby contributing to a reduction in annual energy consumption for air conditioning. Moreover, the increased Th_{win} can also provide better acoustic insulation, contributing to a more comfortable and quieter indoor environment, an aspect particularly valuable in densely populated or urban areas. However, it is essential to balance these benefits with potential downsides, such as the increased weight and cost, which could affect the feasibility and economic viability of installing thicker glass in large-scale applications. In addition, high Th_{win} provides enhanced thermal insulation, reducing the rate of heat transfer from the warm interior to the colder external environment. This improved insulation capability can lead to substantial reductions in heating energy requirements. Overall, the DI of AHC, ACC, ALC, and PPD were respectively 1%, 1%, 0%, and 1%, which means that Th_{win} has a small influence on AHC, ACC, ALC, and PPD.
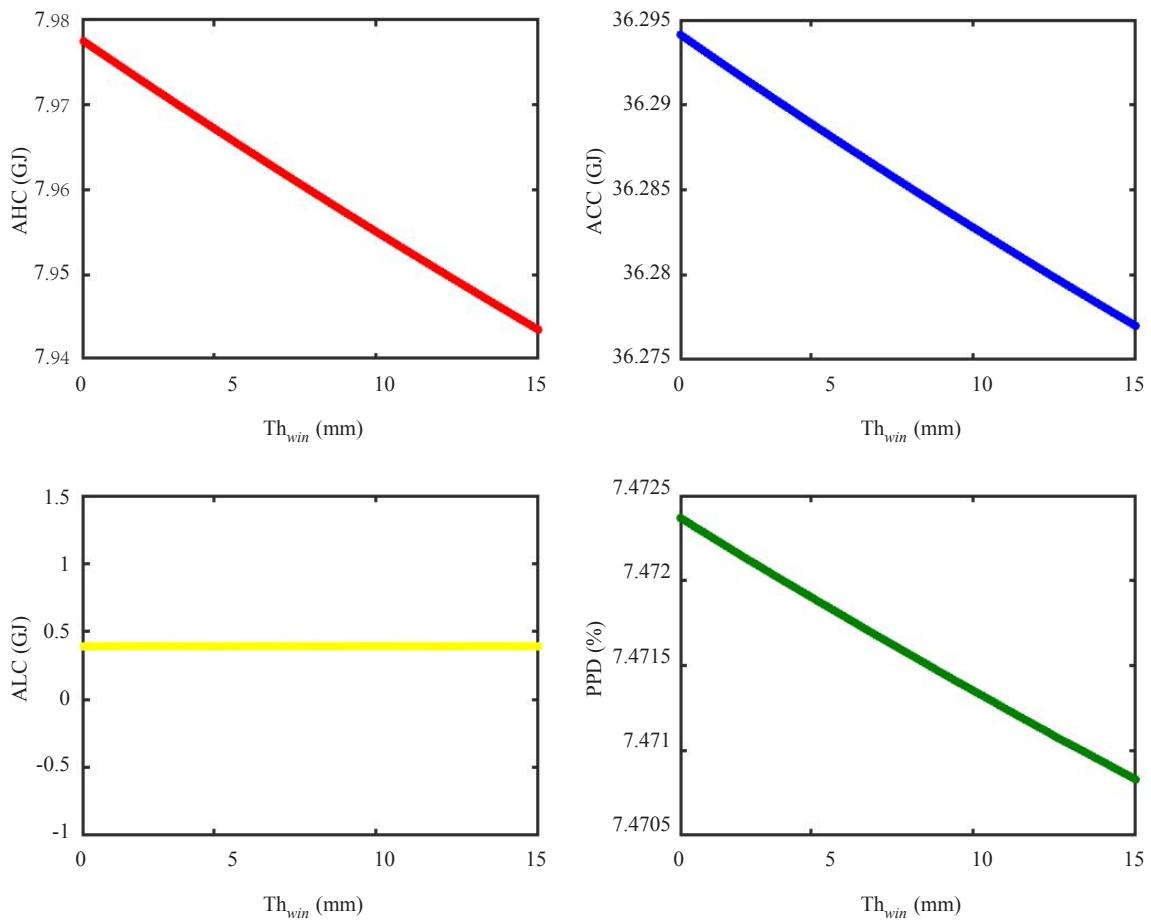
Figure 13. Influence of Th_{win} on the AHC, ACC, ALC, and PPD

4.1.12 *Influence of $Th_{gas-win}$*

Figure 14 indicates the influence of $Th_{gas-win}$ on the AHC, ACC, ALC, and PPD. As observed, with the increase in $Th_{gas-win}$ from 1 mm to 14 mm, the AHC, ACC, and PPD decreased exponentially. However, $Th_{gas-win}$ did not affect the ALC. Enhanced $Th_{gas-win}$, typically achieved by increasing the space between panes and utilizing inert gases improves the thermal insulation of windows. This enhancement reduces thermal conductivity and heat transfer, leading to a notable decrease in cooling energy requirements by minimizing the intrusion of external heat into the building during hot periods. Concurrently, this insulation property helps in retaining interior warmth during cooler times, thereby reducing heating energy demands. High $Th_{gas-win}$ directly contributes to a more stable and comfortable indoor environment, as it minimizes the thermal exchange between the interior and exterior. In winter, the increased $Th_{gas-win}$ helps retain warmth within a room, preventing cold spots and reducing the chill effect near windows, thus ensuring a uniformly comfortable space. Conversely, during the warmer months, this enhanced insulation limits the ingress of external heat, keeping indoor spaces cooler and more comfortable without excessive reliance on air conditioning systems. Furthermore, the reduced need for heating and cooling to maintain thermal comfort not only lowers energy consumption but also mitigates fluctuations in indoor temperatures, leading to a more consistently comfortable environment. This stabilization of indoor temperatures is crucial for occupant well-being, as it prevents the discomfort associated with drastic temperature variations and enables individuals to enjoy their living or working spaces to the fullest. Therefore, the careful consideration of gas thickness in window design emerges as a critical factor in achieving superior thermal comfort, underscoring the importance of advanced glazing technologies in modern architectural practices. Consequently,

the DI of AHC, ACC, ALC, and PPD were respectively 2%, 1%, 0%, and 1%, which means that $Th_{gas\text{-}win}$ has a small influence on AHC, ACC, ALC, and PPD.
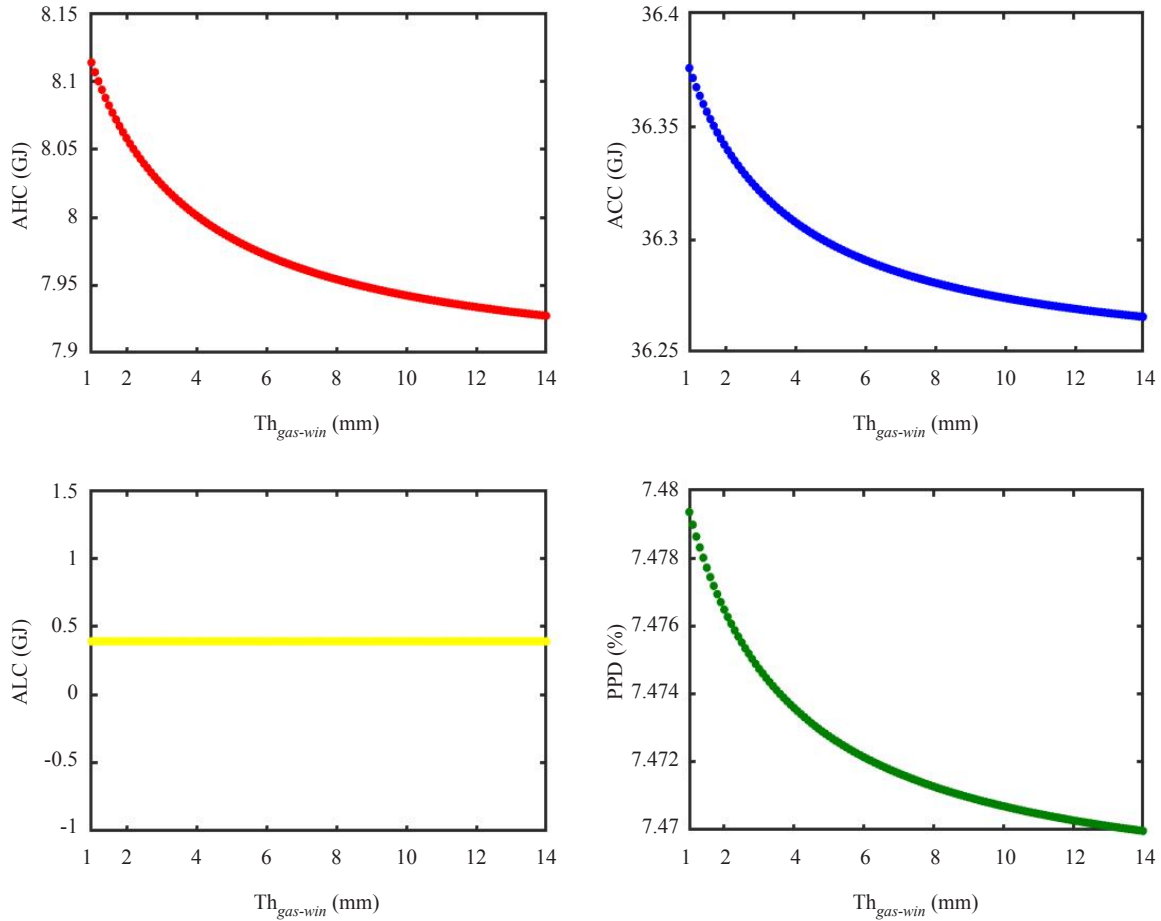

Figure 14. Influence of $Th_{gas\text{-}win}$ on the AHC, ACC, ALC, and PPD

4.2 Results of Sobol's analysis

Table 3 indicates the total-order SI (S_T) as per Sobol's analysis and DI as per OPAT analysis of the AHC, ACC, ALC, and PPD. As observed, HSPT, SA_{Ex_W}, and WWR with the S_T of respectively 80%, 79%, and 35% were the most influential inputs on the AHC while, DSH, CSPT, SA_{IN_W}, ST_{win}, VT_{win}, Th_{win}, and $Th_{gas\text{-}win}$ were the least influential inputs on the AHC. Also, BR and Th_{Ex_W} with the S_T of respectively 16% and 13% had a moderate influence on the AHC. In addition, CSPT, SA_{Ex_W}, and WWR with the S_T of respectively 72%, 63%, and 24% were the most influential inputs on the ACC. However, $Th_{gas\text{-}win}$, SA_{IN_W}, Th_{win}, and VT_{win} were respectively the least influential inputs on the ACC. Further, WWR, VT_{win}, and BR with the S_T of respectively 33%, 25%, and 21% were the most influential inputs on the ALC, while CSPT, HSPT, SA_{IN_W}, SA_{Ex_W}, Th_{Ex_W}, ST_{win}, Th_{win}, and $Th_{gas\text{-}win}$ did not affect the ALC because of the non-dependence of the ALC on specifications of HVAC system and thermo-physical properties of wall and window glass. Additionally, CSPT, HSPT, SA_{Ex_W}, and WWR with the S_T of respectively 81%, 40%, 36%, and 28% were respectively the most influential inputs on the PPD, while other parameters were the least influential inputs on the

PPD. Summery, as per the results of Sobol's analysis, several conclusions were obtained for our building under study as follows:

1. BR had the most influence on the ALC and the least influence on the PPD.
2. WWR had the most influence on the AHC and ALC and the least influence on the ACC.
3. DSH had the most influence on the ALC and the least influence on the PPD.
4. CSPT had the most influence on the ACC and PPD and the least influence on the ALC and AHC.
5. HAPT had the most influence on the AHC and PPD and the least influence on the ALC and ACC.
6. $SA_{\text{Ex\_W}}$ had the most influence on the AHC and the least influence on the ALC.
7. $Th_{\text{Ex\_W}}$ had the most influence on the AHC and the least influence on the ALC.
8. ST_{win}, $SA_{\text{IN\_W}}$, Th_{win}, and $Th_{gas\text{-}win}$ had no impact on the ALC and had very little influence on AHC, ACC, and PPD.
9. VT_{win} had the most influence on the ALC and had very little influence on AHC, ACC, and PPD.
10. AHC had a strong dependence on HSPT and $SA_{\text{Ex\_W}}$.
11. had a strong dependence on CSPT and $SA_{\text{Ex\_W}}$.
12. had a strong dependence on WWR and VT_{win}.
13. had a strong dependence on HSPT and CSPT.
14. ALC had no dependence on the CSPT, HSPT, $SA_{\text{IN\_W}}$, $SA_{\text{Ex\_W}}$, $Th_{\text{Ex\_W}}$, ST_{win}, Th_{win}, and $Th_{gas\text{-}win}$.

Table 3. Total-order SI (S_T) as per Sobol's analysis and DI as per OPAT analysis

Item	Input	AHC		ACC		ALC		PPD	
		S_T(%)	DI(%)	S_T(%)	DI(%)	S_T(%)	DI(%)	S_T(%)	DI(%)
x_1	BR	16	12	6	3	21	8	2	1
x_2	WWR	35	27	24	18	33	28	28	7
x_3	DSH	3	2	4	2	6	2	2	1
x_4	CSPT	2	1	72	54	0	0	81	64
x_5	HSPT	80	92	2	1	0	0	40	22
x_6	$SA_{\text{IN\_W}}$	4	1	3	1	0	0	2	1
x_7	$SA_{\text{Ex\_W}}$	79	63	63	44	0	0	36	20
x_8	$Th_{\text{Ex\_W}}$	13	10	8	6	0	0	4	2
x_9	ST_{win}	7	5	6	4	0	0	2	1
x_{10}	VT_{win}	2	1	2	1	25	11	3	1
x_{11}	Th_{win}	3	1	2	1	0	0	2	1
x_{12}	$Th_{gas\text{-}win}$	2	2	2	1	0	0	3	1

Besides, by comparing the results obtained through the OPAT and Sobol's analyses, it may be concluded that the sensitivity results obtained by the introduced DI in OPAT are in good agreement with Sobol's because the main idea

of defining the DI was taken as per the variance of the output due to changes in the input. Without having an index in OPAT analysis, it was not possible to determine the sensitivity of the outputs to the inputs only by monitoring the OPAT graphs, mainly due to the non-linear behavior of the building system. Therefore, the introduced DI may be used for the OPAT analysis of different systems and obtain reliable results. It should be noted that the ranges adopted for the inputs highly affect the SA results. Therefore, the authors chose the ranges of inputs as per the most common materials in the market as well as the EnergyPlus data set [56].

As can be deduced from the results, both OPAT and Sobol's methods offer unique insights into sensitivity analysis but differ significantly in their approach and the depth of information they provide. The OPAT method, with its straightforward approach of altering one input variable at a time while keeping others constant, offers an intuitive way to identify the influence of individual factors on the output. This method is particularly accessible and easy to implement, making it a popular choice for preliminary sensitivity analyses. However, its major limitation lies in its inability to capture the interactive effects between variables, which can lead to an incomplete understanding of the system being studied.

In contrast, Sobol's method employs a more sophisticated approach based on variance decomposition to quantify the contribution of each input variable to the output's variance, including both the main effects and all possible interactions among variables. This method provides a comprehensive view of the sensitivity landscape, enabling researchers to identify not only the most influential factors but also how these factors interact with each other to affect the system's output. Sobol's method, rooted in the mathematical framework of variance-based sensitivity analysis, offers a more detailed and accurate depiction of the system's behavior, but it requires significantly more computational resources compared to the OPAT method. The choice between OPAT and Sobol's methods should, therefore, be guided by the specific requirements of the study, including the complexity of the model, the number of input variables, the need to understand interaction effects, and the available computational resources.

5. Conclusions

As buildings are inherently very complex multivariable systems, undoubtedly, SBSA is a leading and indispensable approach for building engineers and decision-makers to predict the sensitivity and behavior of the system to its inputs to adopt the best solutions in the shortest possible time. This research introduced a powerful method for SBSA of building performance by integrating EnergyPlus with LSA and GSA algorithms through the C++ programming language. Accordingly, the C++ features and potentials were added into EnergyPlus to perform SBSA of building performance directly without the use of other plugins and third parties. A dwelling house situated in Bushehr (Iran) with a hot semi-arid climate was adopted as a case study to examine the sufficiency of the introduced approach. Hereupon, the building rotation (BR) from the north axis, window-to-wall ratio (WWR), depth of shading device (DSH), cooling and heating setpoints (CSPT and HSPT), solar absorptance of the building walls including interior walls ($SA_{\text{IN\_W}}$) and exterior walls ($SA_{\text{Ex\_W}}$), thickness of (building) wall (Th$_{\text{Ex\_W}}$), solar transmittance of window glass (ST$_{win}$), visible transmittance of window glass (VT$_{win}$), thickness of window glass (Th$_{win}$), thickness of gas in window (Th$_{gas\text{-}win}$) were adopted as input variables. Moreover, four major building criteria including AHC, ACC, ALC, and PPD were adopted as output variables. The OPAT analysis as the LSA and Sobol's analysis as the GSA were conducted to scrutinize the behavior of outputs contrasted to input changes and to quantify the sensitivity of outputs-to-inputs. In the LSA approach, a new sensitivity index was suggested to specify the influence of inputs on outputs. The results demonstrated that for our building under study, AHC was most sensitive to the heating setpoint and solar absorptance of the building exterior walls, respectively. ACC was most sensitive to the cooling setpoint and solar absorptance of the building exterior walls, respectively. Besides, WWR, visible transmittance of window glass, and building rotation were respectively the most influential inputs on the ALC. Furthermore, cooling and heating setpoints, the solar absorptance of the building exterior walls, and WWR were respectively the most influential inputs on the PPD. The CSPT, HSPT, $SA_{\text{IN\_W}}$, $SA_{\text{Ex\_W}}$, Th$_{\text{Ex\_W}}$, ST$_{win}$, Th$_{win}$, and Th$_{gas\text{-}win}$ did not affect the ALC. Furthermore, the proposed DI was in good agreement with the S_T. It was deduced the design specifications remarkably affected building efficiency in such a way that with reasonable adoption of parameters, it is possible to achieve a building that has the lowest energy loss and the highest resident's thermal comfort. By carefully considering the local climate and building orientation, and incorporating appropriate materials, colors, and

architectural strategies, it is possible to optimize the energy efficiency of buildings while ensuring a comfortable living and working environment.

Additionally, the results showed that OPAT provides a quick and straightforward way to identify influential factors. It requires fewer model runs, which can be advantageous when dealing with computationally expensive models, and is effective for identifying the direct impact of each input variable on the output. However, OPAT does not account for interaction effects between variables. In many complex systems with a large number of input variables like building, the output depends on the interaction between two or more inputs, which OPAT fails to capture. Because it doesn't consider interactions, OPAT might lead to misleading conclusions about the importance of variables or their impact on the system. On the other hand, Sobol's method delivered a comprehensive and nuanced understanding of the system's sensitivity dynamics, making it invaluable for complex models where interactions play a significant role in determining the output. Nonetheless, Sobol's method requires a significant number of model runs, making it computationally expensive.

The developed approach prepared a speedy and accurate way to perform the SBSA of buildings during the design phase by integrating the abilities of LSA and GSA algorithms into EnergyPlus and prepared an opportunity for building engineers to have a better picture of the range of options for decision-making. Consequently, the introduced SBSA approach allows building designers and decision-makers to identify the significant parameters to design a building with optimal performance by carefully adopting the best elements at the initial conceptual design phase in the shortest possible time.

Our future investigation involves multi-objective optimization of the building under study to extract the Pareto optimal solutions and determine the trade-off between building energy use and residents' thermal comfort. In addition, the proposed method will be implemented in different climate zones of Iran to examine the influences of climate on building efficiency. It would be also interesting to examine the introduced procedure on other building types, particularly net zero energy buildings. Besides, the SBSA of acoustic comfort and respiratory comfort, environmental and economic analysis, embodied energy, and life cycle assessment should be performed to get more robust design results.

Data availability statements

All data generated or analyzed during this study are included in this published article.

Conflict of interest

The authors declare no competing financial interest.

References

[1] H. Ramin, P. Hanafizadeh, and M. A. Akhavan-Behabadi, "Determination of optimum insulation thickness in different wall orientations and locations in Iran," *Advances in Building Energy Research*, vol. 10, no. 2, pp. 149-171, 2016. Available: https://doi.org/10.1080/17512549.2015.1079239.

[2] M. Nasouri, and N. Delgarm, "Bushehr Nuclear Power Plants (BNPPs) and the perspective of sustainable energy development in Iran," *Progress in Nuclear Energy*, vol. 147, no. 12, pp. 104179, 2022. Available: https://doi.org/10.1016/j.pnucene.2022.104179.

[3] "Detailed statistical report on 55 years of activities of Iran electric power industry" (in Persian), Tavanir Organization, (1967-2021), Iran, 2021.

[4] "Energy balance sheet" (in Persian), Office of planning and macroeconomics of electricity and energy, Ministry of Energy, Iran, 2021.

[5] N. Delgarm, B. Sajadi, K. Azarbad, and S. Delgarm, "Sensitivity analysis of building energy performance: A simulation-based approach using OFAT and variance-based sensitivity analysis methods," *Journal of Building Engineering*, vol. 15, pp. 181-193, 2018. Available: https://doi.org/10.1016/j.jobe.2017.11.020.

[6] N. Delgarm, B. Sajadi, F. Kowsary, and S. Delgarm, "Multi-objective optimization of the building energy

performance: A simulation-based approach by means of particle swarm optimization (PSO)," *Applied Energy*, vol. 170, pp. 293-303, 2016. Available: https://doi.org/10.1016/j.apenergy.2016.02.141.

[7] P. Lotfabadi, and P. Hançer, "Optimization of visual comfort: Building openings," *Journal of Building Engineering*, vol. 72, pp. 106598, 2023. Available: https://doi.org/10.1016/j.jobe.2023.106598.

[8] N. Delgarm, B. Sajadi, and S. Delgarm, "Multi-objective optimization of building energy performance and indoor thermal comfort: A new method using artificial bee colony (ABC)," *Energy and Buildings*, vol. 131, pp. 42-53, 2016. Available: https://doi.org/10.1016/j.enbuild.2016.09.003.

[9] H. Wang, C. Lin, Y. Hu, X. Zhang, J. Han, and Y. Cheng, "Study on indoor adaptive thermal comfort evaluation method for buildings integrated with semi-transparent photovoltaic window," *Building and Environment*, vol. 228, pp. 109834, 2023. Available: https://doi.org/10.1016/j.buildenv.2022.109834.

[10] P. Zheng, H. Wu, Y. Liu, Y. Ding, and L. Yang, "Thermal comfort in temporary buildings: A review," *Building and Environment*, vol. 221, pp. 109262, 2022. Available: https://doi.org/10.1016/j.buildenv.2022.109262.

[11] "ANSI/ASHRAE Standard 55-2010-Thermal Environmental Conditions for Human Occupancy", Atlanta: American Society of Heating, Refrigerating, and Air-Conditioning Engineers, Inc., 2010. Available: https://lorisweb.com/CMGT235/DIS06/ASHRAE-55-2010.pdf.

[12] M. Charai, A. Mezrhab, and L. Moga, "A structural wall incorporating biosourced earth for summer thermal comfort improvement: Hygrothermal characterization and building simulation using calibrated PMV-PPD model," *Building and Environment*, vol. 212, pp. 108842, 2022. Available: https://doi.org/10.1016/j.buildenv.2022.108842.

[13] P. O. Fanger, *Thermal Comfort: Analysis and Applications in Environmental Engineering*. Copenhagen: Danish Technical Press, 1970, pp. 244.

[14] L. Junghans, and N. Darde, "Hybrid single objective genetic algorithm coupled with the simulated annealing optimization method for building optimization," *Energy and Buildings*, vol. 86, pp. 651-662, 2015. Available: https://doi.org/10.1016/j.enbuild.2014.10.039.

[15] E. M. Salilih, N. H. Abu-Hamdeh, A. B. Khoshaim, R. A. Almasri, S. M. Sajadi, and A. Karimipour, "Thermal systems energy optimization employing two independent circuits of double vertical ground U-tube with PCM as the backfill material for building," *Journal of Building Engineering*, vol. 56, pp. 104752, 2022. Available: https://doi.org/10.1016/j.jobe.2022.104752.

[16] N. Delgarm, B. Sajadi, S. Delgarm, and F. Kowsary, "A novel approach for the simulation-based optimization of the buildings energy consumption using NSGA-II: Case study in Iran," *Energy and Buildings*, vol. 127, pp. 552-560, 2016. Available: https://doi.org/10.1016/j.enbuild.2016.05.052.

[17] X. Zhu, X. Zhang, P. Gong, and L. Yu, "A review of distributed energy system optimization for building decarbonization," *Journal of Building Engineering*, vol. 73, pp. 106735, 2023. Available: https://doi.org/10.1016/j.jobe.2023.106735.

[18] Q. Wang, G. Chen, M. Khishe, B. F. Ibrahim, and S. Rashidi, "Multi-objective optimization of IoT-based green building energy system using binary metaheuristic algorithms," *Journal of Building Engineering*, vol. 68, pp. 106031, 2023. Available: https://doi.org/10.1016/j.jobe.2023.106031.

[19] G. Aruta, F. Ascione, N. Bianco, G. M. Mauro, and G. P. Vanoli, "Optimizing heating operation via GA- and ANN-based model predictive control: Concept for a real nearly-zero energy building," *Energy and Buildings*, vol. 292, pp. 113139, 2023. Available: https://doi.org/10.1016/j.enbuild.2023.113139.

[20] Y. Pan, M. Zhu, Y. Lv, Y. Yang, Y. Liang, R. Yin, Y. Yang, X. Jia, X. Wang, F. Zeng, S. Huang, D. Hou, L. Xu, R. Yin, and X. Yuan, "Building energy simulation and its application for building performance optimization: A review of methods, tools, and case studies," *Advances in Applied Energy*, vol. 10, pp. 100135, 2023. Available: https://doi.org/10.1016/j.adapen.2023.100135.

[21] A. T. Nguyen, S. Reiter, and P. Rigo, "A review on simulation-based optimization methods applied to building performance analysis," *Applied Energy*, vol. 113, pp. 1043-1058, 2014. Available: https://doi.org/10.1016/j.apenergy.2013.08.061.

[22] M. Shin, and J. S. Haberl, "A procedure for automating thermal zoning for building energy simulation," *Journal of Building Engineering*, vol. 46, pp. 103780, 2022. Available: https://doi.org/10.1016/j.jobe.2021.103780.

[23] C. Carpino, R. Bruno, V. Carpino, and N. Arcuri, "Uncertainty and sensitivity analysis to moderate the risks of energy performance contracts in building renovation: A case study on an Italian social housing district," *Journal of Cleaner Production*, vol. 379, pp. 134637, 2022. Available: https://doi.org/10.1016/j.jclepro.2022.134637.

[24] A. Saurbayeva, S. A. Memon, and J. R. Kim, "Integrated multi-stage sensitivity analysis and multi-objective optimization approach for PCM integrated residential buildings in different climate zones," *Energy*, vol. 278, pp. 127973, 2023. Available: https://doi.org/10.1016/j.energy.2023.127973.

[25] V. F. Mendes, W. Fardin, R. R. Barreto, L. F. Caetano, and J. C. Mendes, "Sensitivity analysis of coating mortars

according to their specific heat, specific gravity, thermal conductivity, and thickness in contribution to the global thermal performance of buildings," *Sustainable Materials and Technologies*, vol. 31, pp. e00381, 2022. Available: https://doi.org/10.1016/j.susmat.2021.e00381.

[26] D. Liu, P. Jiang, H. Chen, and T. Yan, "Comparison of local and global sensitivity analysis methods and application to thermal hydraulic phenomena," *Progress in Nuclear Energy*, vol. 158, pp. 104612, 2023. Available: https://doi.org/10.1016/j.pnucene.2023.104612.

[27] F. Rentzeperis, and D. Wallace, "Local and global sensitivity analysis of spheroid and xenograft models of the acid-mediated development of tumor malignancy," *Applied Mathematical Modelling*, vol. 109, pp. 629-650, 2022. Available: https://doi.org/10.1016/j.apm.2022.05.006.

[28] S. P. Saha, S. Ghosh, D. Mazumdar, S. Ghosh, D. Ghosh, M. M. Sarkar, and S. Roy, "Valorization of banana peel into α-amylase using one factor at a time (OFAT) assisted artificial neural network (ANN) and its partial purification, characterization, and kinetics study," *Food Bioscience*, vol. 53, pp. 102533, 2023. Available: https://doi.org/10.1016/j.fbio.2023.102533.

[29] S. P. Saha, and D. Mazumdar, "Optimization of process parameter for alpha-amylase produced by Bacillus cereus amy3 using one factor at a time (OFAT) and central composite rotatable (CCRD) design based response surface methodology (RSM)," *Biocatalysis and Agricultural Biotechnology*, vol. 19, pp. 101168, 2019. Available: https://doi.org/10.1016/j.bcab.2019.101168.

[30] B. Xu, S. Wang, H. Xia, Z. Zhu, and X. Chen, "A global sensitivity analysis method for safety influencing factors of RCC dams based on ISSA-ELM-Sobol," *Structures*, vol. 51, pp. 288-302, 2023. Available: https://doi.org/10.1016/j.istruc.2023.03.027.

[31] B. Vuillod, M. Montemurro, E. Panettieri, and L. Hallo, "A comparison between Sobol's indices and Shapley's effect for global sensitivity analysis of systems with independent input variables," *Reliability Engineering & System Safety*, vol. 234, pp. 109177, 2023. Available: https://doi.org/10.1016/j.ress.2023.109177.

[32] Y. Zhang, X. Zhang, P. Huang, and Y. Sun, "Global sensitivity analysis for key parameters identification of net-zero energy buildings for grid interaction optimization," *Applied Energy*, vol. 279, pp. 115820, 2020. Available: https://doi.org/10.1016/j.apenergy.2020.115820.

[33] Z. Kala, "Global sensitivity analysis based on entropy: From differential entropy to alternative measures," *Entropy*, vol. 23, no. 6, pp. 778, 2021. Available: https://doi.org/10.3390/e23060778.

[34] F. K. Zadeh, J. Nossent, F. Sarrazin, F. Pianosi, A. van Griensven, T. Wagener, and W. Bauwens, "Comparison of variance-based and moment-independent global sensitivity analysis approaches by application to the SWAT model," *Environmental Modelling and Software*, vol. 91, pp. 210-222, 2017. Available: https://doi.org/10.1016/j.envsoft.2017.02.001.

[35] F. Pianosi, and T. Wagener, "A simple and efficient method for global sensitivity analysis based on cumulative distribution functions," *Environmental Modelling and Software*, vol. 67, pp. 1-11, 2015. Available: https://doi.org/10.1016/j.envsoft.2015.01.004.

[36] A. Saltelli, and I. Sobol, "Sensitivity analysis for nonlinear mathematical models. numerical experience," *Matematicheskoe Modelirovanie*, vol. 7, no. 11, pp. 16-28, 1995. Available: https://publications.jrc.ec.europa.eu/repository/handle/JRC11279.

[37] S. Lo Piano, F. Ferretti, A. Puy, D. Albrecht, and A. Saltelli, "Variance-based sensitivity analysis: The quest for better estimators and designs between explorativity and economy," *Reliability Engineering & System Safety*, vol. 206, pp. 107300, 2021. Available: https://doi.org/10.1016/j.ress.2020.107300.

[38] Z. Xy, T. Mn, L. Lj, and S. Schmidt, "SOBOL Sensitivity Analysis: a tool to guide the development and evaluation of systems pharmacology models," *CPT: Pharmacometrics & Systems Pharmacology*, vol. 4, no. 2, pp. 69-79, 2015. Available: https://doi.org/10.1002/psp4.6.

[39] A. Saltelli, M. Ratto, T. Andres, F. Campolongo, J. Cariboni, D. Gatelli, M. Saisana, and S. Tarantola, *Global Sensitivity Analysis: The Primer*. Wiley-Interscience, 2008.

[40] Z. Pang, Z. O'Neill, Y. Li, and F. Niu, "The role of sensitivity analysis in the building performance analysis: A critical review," *Energy and Buildings*, vol. 209, pp. 109659, 2020. Available: https://doi.org/10.1016/j.enbuild.2019.109659.

[41] Y. Shen, and M. Yarnold, "A novel sensitivity analysis of commercial building hybrid energy-structure performance," *Journal of Building Engineering*, vol. 43, pp. 102808, 2021. Available: https://doi.org/10.1016/j.jobe.2021.102808.

[42] D. Maučec, M. Premrov, and V. Ž. Leskovar, "Use of sensitivity analysis for a determination of dominant design parameters affecting energy efficiency of timber buildings in different climates," *Energy for Sustainable Development*, vol. 63, pp. 86-102, 2021. Available: https://doi.org/10.1016/j.esd.2021.06.003.

[43] S. Yang, F. Fiorito, D. Prasad, A. B. Sproul, and A. Cannavale, "A sensitivity analysis of design parameters of BIPV/T-DSF in relation to building energy and thermal comfort performances," *Journal of Building Engineering*, vol. 41, pp. 102426, 2021. Available: https://doi.org/10.1016/j.jobe.2021.102426.

[44] H. Huo, W. Xu, A. Li, J. Chu, and Y. Lv, "Sensitivity analysis and prediction of shading effect of external Venetian blind for nearly zero-energy buildings in China," *Journal of Building Engineering*, vol. 41, pp. 102401, 2021. Available: https://doi.org/10.1016/j.jobe.2021.102401.

[45] J. Goffart, and M. Woloszyn, "EASI RBD-FAST: An efficient method of global sensitivity analysis for present and future challenges in building performance simulation," *Journal of Building Engineering*, vol. 43, pp. 103129, 2021. Available: https://doi.org/10.1016/j.jobe.2021.103129.

[46] J. Chambers, M. J. S. Zuberi, K. N. Streicher, and M. K. Patel, "Geospatial global sensitivity analysis of a heat energy service decarbonisation model of the building stock," *Applied Energy*, vol. 302, pp. 117592, 2021. Available: https://doi.org/10.1016/j.apenergy.2021.117592.

[47] S. Yip, A. Athienitis, and B. Lee, "Early stage design for an institutional net zero energy archetype building. Part 1: Methodology, form and sensitivity analysis," *Solar Energy*, vol. 224, pp. 516-530, 2021. Available: https://doi.org/10.1016/j.solener.2021.05.091.

[48] V. Zeferina, F. Wood, R. Edwards, and W. Tian, "Sensitivity analysis of cooling demand applied to a large office building," *Energy and Buildings*, vol. 235, pp. 110703, 2021. Available: https://doi.org/10.1016/j.enbuild.2020.110703.

[49] S. Naji, L. Aye, and M. Noguchi, "Sensitivity analysis on energy performance, thermal and visual discomfort of a prefabricated house in six climate zones in Australia," *Applied Energy*, vol. 298, pp. 117200, 2021. Available: https://doi.org/10.1016/j.apenergy.2021.117200.

[50] A. Bozzhigitov, S. A. Memon, and I. Adilkhanova, "Sensitivity of energy performance to the selection of PCM melting temperature for the building located in Cfb climate zone," *Energy Reports*, vol. 8, pp. 6301-6320, 2022. Available: https://doi.org/10.1016/j.egyr.2022.04.059.

[51] L. Zhu, J. Zhang, Y. Gao, W. Tian, Z. Yan, X. Ye, Y. Sun, and C. Wu "Uncertainty and sensitivity analysis of cooling and heating loads for building energy planning," *Journal of Building Engineering*, vol. 45, pp. 103440, 2022. Available: https://doi.org/10.1016/j.jobe.2021.103440.

[52] Y. Zhang, X. Zhang, P. Huang, and Y. Sun, "Global sensitivity analysis for key parameters identification of net-zero energy buildings for grid interaction optimization," *Applied Energy*, vol. 279, pp. 115820, 2020. Available: https://doi.org/10.1016/j.apenergy.2020.115820.

[53] J. Mukkavaara, and F. Shadram, "An integrated optimization and sensitivity analysis approach to support the life cycle energy trade-off in building design," *Energy and Buildings*, vol. 253, pp. 111529, 2021. Available: https://doi.org/10.1016/j.enbuild.2021.111529.

[54] A. Saltelli, S. Tarantola, F. Campolongo, and M. Ratto, *Sensitivity Analysis in Practice: A Guide to Assessing Scientific Models*. John Wiley, 2004. Available: http://ci.nii.ac.jp/ncid/BA68804524.

[55] A. Saltelli, P. Annoni, I. Azzini, F. Campolongo, M. Ratto, and S. Tarantola, "Variance based sensitivity analysis of model output. Design and estimator for the total sensitivity index," *Computer Physics Communications*, vol. 181, no. 2, pp. 259-270, 2010. Available: https://doi.org/10.1016/j.cpc.2009.09.018.

[56] "EnergyPlus V 23.1.0." Available: https://energyplus.net/.

[57] "SketchUp V 2023.0.1." Available: https://www.sketchup.com/.

[58] EPA, *A Guide to Energy-Efficient Heating and Cooling*. United States Environmental Protection Agency (EPA), Washington, D. C., USA, 2009. Available: https://www.energystar.gov/ia/partners/publications/pubdocs/HeatingCoolingGuide%20FINAL_9-4-09.pdf.

[59] International Commission on Illumination, *Light and lighting-Lighting of work places-Part 1: Indoor work places*. EN 12464-1, European Committee for Standardization, Brussels, Belgium, 2011. Available: https://cie.co.at/publications/light-and-lighting-lighting-work-places-part-1-indoor.

[60] M. Nasouri, and N. Delgarm, "Numerical modeming, energy-exergy analyses, and multi-objective programming of the solar-assisted heat pump system using genetic algorithm coupled with the multi-criteria decision analysis," *Arabian Journal for Science and Engineering*, vol. 48, no. 3, pp. 3537-3557, 2021. Available: https://doi.org/10.1007/s13369-022-07151-3.

[61] M. Nasouri, G. N. Bidhendi, M. J. Amiri, N. Delgarm, S. Delgarm, and K. Azarbad, "Performance-based Pareto optimization and multi-attribute decision making of an actual indirect-expansion solar-assisted heat pump system," *Journal of Building Engineering*, vol. 42, pp. 103053, 2021, Available: https://doi.org/10.1016/j.jobe.2021.103053.

[62] H. Tao, N. Delgarm, D. Wang, and M. Karimi, "Energy, economic, and environmental (3E) examinations of the indirect-expansion solar heat pump water heater system: A simulation-oriented performance optimization and

multi-objective decision-making," *Journal of Building Engineering*, vol. 60, pp. 105068, 2022. Available: https://doi.org/10.1016/j.jobe.2022.105068.

[63] "Bushehr Meteorological Station Report Data Processing Center", The Iran Meteorological Administration, (2019-2023), Iran, 2024.

[64] M. Nasouri, and N. Delgarm, "Efficiency-based Pareto optimization of building energy consumption and thermal comfort: A case study of a residential building in Bushehr, Iran," *Journal of Thermal Science*, pp. 1-18, 2023. Available: https://doi.org/10.1007/s11630-023-1933-5.

[65] M. Nasouri, and N. Delgarm, "Investigating the role of Bushehr Nuclear Power Plants (BNPPs) in line with achieving the perspective of sustainable energy development in Iran," *Journal of Thermal Science*, vol. 31, no. 5, pp. 1392-1406, 2022. Available: https://doi.org/10.1007/s11630-022-1576-y.

[66] "Ashrae climatic design conditions 2009/2013/2017/2021". Available: http://ashrae-meteo.info/v2.0/?lat=28.9036&lng=50.8208&place=%27%27&wmo=408570&si_ip=SI&ashrae_version=2021.

[67] S.-W. Yu, S. Hao, J. Mu, and D. Tian, "Optimization of wall thickness based on a comprehensive evaluation index of thermal mass and insulation," *Sustainability*, vol. 14, no. 3, pp. 1143, 2022. Available: https://doi.org/10.3390/su14031143.